INTERNATIONAL ATOMIC ENERGY AGENCY

INDC(NDS)-419
Distr.: L0+ND

I N D C   INTERNATIONAL NUCLEAR DATA COMMITTTEE

SELECTED ARTICLES TRANSLATED FROM
JADERNYE KONSTANTY (NUCLEAR CONSTANTS)

(Series: Nuclear Constants Issue No. 2, 1998

Translated by the IAEA

April 1999

_____

IAEA NUCLEAR DATA SECTION, WAGRAMERSTRASSE 5, A-1400 VIENNA

**SELECTED ARTICLES TRANSLATED FROM
JADERNYE KONSTANTY (NUCLEAR CONSTANTS)**

(Series: Nuclear Constants Issue No. 2, 1998)

Translated by the IAEA

April 1999

TABLE OF CONTENTS

SERIYA: YADERNYE KONSTANTY, Vypusk 2, 1998, s. 75
(Series: Nuclear Constants, Issue No. 2, 1998, p.75)

EVALUATION OF THE DECAY CHARACTERISTICS OF ^{3}H AND ^{36}CL

V.P. Chechev

V.G. Khlopin Radium Institute, St. Petersburg

DECAY DATA EVALUATIONS FOR ^{3}H AND ^{36}Cl. Decay data of the radionuclides ^{3}H and ^{36}Cl have been evaluated using the information published up to 1998.

1.   Introduction

This article has been prepared as part of the workplan of the Radionuclide Data Centre at the V.G. Khlopin Radium Institute at the request of the Department for Nuclear Science and Engineering Research at the Ministry of the Russian Federation for Atomic Energy. The article presents the results of evaluation of the decay data of the radionuclides ^{3}H and ^{36}Cl, and of their atomic and nuclear characteristics, using the information published up to 1998. The work was carried out within the framework of the international project on decay data evaluation for widely used radionuclides: DDEP (Decay Data Evaluation Project)[*]. The number of such radionuclides is estimated to be approximately 300, and under the DDEP, it was agreed to distribute them among various groups participating in the project with subsequent expert assessment of the evaluations by all participants. At present, representatives of eight nuclear metrological laboratories from the United Kingdom, Germany, Spain, Russia and the United States of America are participating in the project. The project co-ordinator is Dr. Helmer from the Idaho National Engineering Laboratory (INEL). The Radionuclide Data Centre at the Radium Institute was given the task of evaluating the decay and radiation characteristics of the radionuclides ^{3}H, ^{14}C, ^{32}P, ^{35}S,

---

[*]   R.G. Helmer. International Decay Data Project. Proceedings of the International Symposium "Advances in α, β and γ-ray Spectrometry", Pushkin (St. Petersburg, Russia), September 1996, CIEMAT, Madrid, 1997, p. 71.
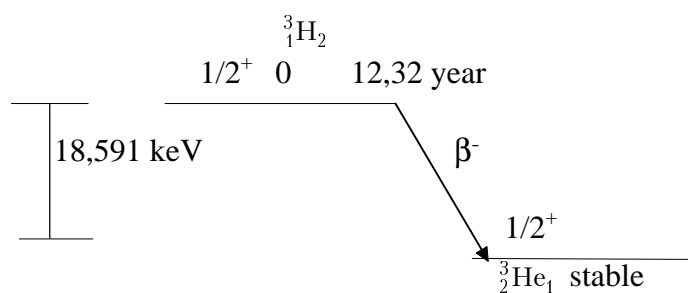
^{36}Cl and ^{111}In in 1997-98. Accordingly, this article presents the results of the evaluation of the characteristics of two of the six above-mentioned radionuclides.

2. Evaluation of the data for ^{3}H

The results of the evaluation of the nuclear and atomic data for the radionuclide ^{3}H using information published up to 1998 are given below. The errors of these values are given in brackets in units of the last significant order of magnitude. The results of the evaluation are presented in the format adopted by the participants of the international co-operation project DDER.

2.1. Decay diagram

100% of ^{3}H is converted by the β-decay directly to the fundamental state of ^{3}He.

$$^3_1H_2$$

$1/2^+$ 0   12,32 year

18,591 keV   β$^-$

$1/2^+$

$^3_2He_1$ stable

2.2. Nuclear data

T$_{½}$:   12.32 (2) years
Q$_{β}$-:   18.591 (2) keV

2.2.1. β$^-$-transition

	Energy, keV	Probability P$_{β}$-	Nature	lg ft
β$^-$	18.591(2)	1	Allowed	3.05

2.3. Electron emission

	Boundary energy, keV	Average decay energy, keV	Number of electrons per 100 disintegrations
β$^-$	18.564(3)$^{+)}$	5.68(1)	100

$^{+)}$ Calculated for a tritium atom: commentary, see Section 2.4.3.

2.4. *Substantiation of the evaluated values obtained for the decay characteristics of ^3H*

2.4.1. *Half-life*

Many measurements of the half-life of tritium have been presented in the literature [1-17] (see Table 2.1). Three of these stand out for their high level of accuracy [6, 9, 11]. However, in their studies, the errors indicated for $T_{1/2}(^3H)$, do not include an evaluation of the possible systematic errors of the methods used. Today, with the benefit of later measurements and discussions of the half-life of tritium, it is possible to evaluate the "external" minimum error of the measurement method as a result of systematic effects (σ_{min}), which should be added to the errors given in Refs [6, 9, 11]. Such an addition to the weighting of all the existing results of the measurements of tritium half-life is necessary in view of the following:

(a) The result of the measurement $T_{1/2}(^3H)$ by accumulating ^3He [6] was obtained using only two points on each decay curve (for two samples). In a later study carried out using the same method [10], many experimental points were obtained on the decay curves (also for two samples) and the evaluated systematic error was 0.6% for a confidence level $P = 99.7\%$, i.e. 0.2% for $P = 0.68$;

(b) Reference [11] was a continuation of the measurements of Ref. [9] using the calorimetric method for two solid tritides over an additional 12 years. The relative difference in the results was 0.2% ($P = 0.68$) - more than 5 σ_{exp} [11] and 10 σ_{exp} [9];

(c) A comparative analysis of measurements of the radioactive concentrations of solutions in some NBS tritiated water standards over an 18-year period 1961-1978 [12] showed that for agreement of the measurements (with a given tritium half-life), their evaluated standard errors (including those for the calorimetric method) should not be less than 0.2%.

Thus, we have sufficient grounds for adding to the errors given in Refs [6, 9, 11] the "external" systematic error $\sigma_{min} = 0.002 - T_{1/2}(^3H)$.

Table 3.2 shows a set of data "1" which was generated from set "0" by omitting the results of two earlier studies with large errors [1, 2] and increasing the errors of Refs [6, 9, 11] up to ±0.25 years.

In addition, the result of Ref. [13], which was refined later in Ref. [17], was omitted, and the weighted mean of measurements [14, 16], performed by the same authors by observing the growth of ^3He, was used for the statistical treatment.

The next step in the selection of data ("1" → "2") is linked to the use of the statistical value X^2 [18]. As none of the experimental results for set "1" lead to a significant increase in the value of X^2, the sets of data "1" and "2", as well as set "3", which is formed after verifying the relative statistical weights of the results (LWM, see [18, 19]), are in agreement.

<u>Table 2.1.</u>: Results of the measurements of tritium half-life (data "0" set)

Reference		Half-life $T_{1/2}(\sigma)$, years	Method	Comments assigned on the error[1]
No.	NSR-ref			
1	40On[**][a]	31(8)	Beta count	
2	47Go08	10.7(20)	Decrease in the ionization current	
3	47No01	12.1(5)	^{3}He accumulation	Error of the mean of the results of measurements for two samples
4	50Je60	12.46(10)	^{3}He diffusion	σ_{syst} included [d]
5	51Jo15	12.41(7) [b]	Beta count	σ_{syst} included [d]
6	55Jo20	12.262(4)	^{3}He accumulation	Error of the measurement for each of the two samples
7	58Po64	12.58(18)	Calorimetry	σ_{syst} included
8	66Me[**][a]	12.31(13)	Absolute count	See [20]
9	67Jo09	12.346(2)	Calorimetry	Probable error in the external agreement of the measurements of six samples
10	67Jo10	12.25(3) [c]	^{3}He accumulation	σ_{syst} included [d]
11	77RuZZ	12.3232(43)	Calorimetry	See text
12	80Un[**][a]	12.43(5)	Comparison of tritium standards	σ_{syst} included [d]
13	87Bu[**][a]	12.29(10)	Beta count	See [20]
14	87Ol04	12.38(3)	^{3}He accumulation	σ_{syst} included [d]
15	875i01	12.32(3)	Implantation of ^{3}H in Si(Li)	σ_{syst} included [d]
16	89Ol[**][a]	12.38(3)	^{3}He accumulation	σ_{syst} included [d]
17	91Bu13	12.31(3)	Bremsstrahlung	σ_{syst} included [d]

a   NSR reference not found.
b   The limits +0.15 -0.25 are given in 50Jo15; σ is calculated in 87Si01.
c   The error +0.08 is quoted in 67Jo10 for a confidence level 99.7%.
d   This denotes allowance for the contribution of possible components of the systematic error in the total error stated by the authors.

By comparing $X^2=26.75$ for the whole set of data (n=13) with the tabulated $(X^2)_{n-1}^{0.05} = 21.0$, we can observe that there is only a small inconsistency in the data, and can use the WM, tS [18] or MBAYS [19] methods for the statistical treatment of data to obtain the recommended value, taking into account the independence of the measurements in Refs [3-17], performed using different methods. It should be noted that the UNIF, PINF, BAYS and NORM procedures give the same result for the recommended value for tritium half-life: $T_{1/2} =12.32(2)$ years (see Table 2.3). The recommended value is given to two decimal places, since the vast majority of processed experimental data do not have a third decimal place.

Table 2.2.   Selected results of the Measurements of Tritium Half-life (set "1" = set "2" = set "3")

Year	Half-life $T_{1/2}(\sigma)$, years	Reference	
		No.	NSR-figure
1947	12.1(5)	3	47No01
1950	12.46(10)	4	50Je60
1951	12.41(7)	5	51Jo15
1955	12.262(25)[a]	6	55Jo20
1958	12.58(18)	7	58Po64
1966	12.31(13)	8	66Me**
1967	12.346(25)[a]	9	67Jo09
1967	12.25(3)	10	67Jo10
1977	12.323(25)[a]	11	77RuZZ
1980	12.43(5)	12	80Un**
1987, 1989	12.38(3)[b]	14,16	87Ol04, 89Ol**
1987	12.32(3)	15	87Si01
1991	12.31(3)	17	91Bu13

a   Error taken as equal to 0.002 $T_{1/2}$, see text.
b   Weighted mean of the results of the measurements 12.38(3) (87Ol04) and 12.38(4) (89Ol**).

Table 2.3.: Results of the Data Treatment using various Statistical Procedures, and Recommended Value of $T_{1/2}(^3H)$

Procedure	Half-life (in years)	Error (in years)
UWM	0.12345E+02	0.32088E-01
WM	0.12321E+02	0.99788E-02
CHV	0.12346E+02	0.20309E-01
UINF	0.12321E+02	0.14899E-01
PINF	0.12321E+02	0.14899E-01
BAYS	0.12321E+02	0.16322E-01
MBAYS	0.12321E+02	0.15562E-01
LWM	0.12321E+02	0.14899E-01
LEXW	0.12333E+02	0.18600E-01
NORM	0.12321E+02	0.14899E-01
RAJ	0.12333E+02	0.10900E-01
WM, min	0.12322E+02	0.25000E-01
WM, tS	0.12322E+02	0.16320E-01
Recommended value	12.32 ± 0.02 years	

2.4.2. Tritium decay energy (Q_{β^-})

G. Audi and A.H. Wapstra [21] recommend a value of 18.591(1) keV for the difference in mass of ^{3}H-^{3}He ($\triangle Mc^2 = Q_{\beta^-}$), using measurements performed with different methods between 1985 and 1993. Table 2.4 shows the results of the measurements of Q_{β^-} as they were given in Ref. [39], with the addition of 83De47 and new references [41-44] up to 1995.

Table 2.4.: Recent measurements of the difference in mass of ^{3}H-^{3}He

Mc^2 (eV)	Method	Year	Reference	
			No.	NSR-figure
18590(10)	Radio frequency mass spectrometry	1975	22	75Sm02
18579(12)	Radio frequency mass spectrometry	1981	23	81Sm02
18575(7)	Implantation in Si(Li)	1983	24	83De47
18584(4)	Ion cyclotron resonance doublet	1984	25	84Ni16
18599(2)	Ion cyclotron resonance doublet	1985	26	85L102
18582(3)	Ion cyclotron resonance doublet	1985	27	85Ta2K
18590(8)	Implantation in Si(Li)	1985	28	85Si07
18581(3)	Ion cyclotron resonance doublet	1986	29	86Go** [a]
18603(10)	Beta spectrometry	1986	30	86Fr09
18599(4)	Beta spectrometry	1987	31	87Bo07
18603(5)	Beta spectrometry	1987	32	87Ka** [a]
18586(6)	Implantation in Si (Li)	1988	33	88BrZN
18589.0(26)	Beta spectrometry	1989	34	89St05
18595(6)	Bremsstrahlung	1991	35	91Bu12
18590.6(20)	Beta spectrometry	1991	36	91Ro07
18590.9(30)	Beta spectrometry	1991	37	91Ka41
18591.0(20)	Beta spectrometry	1992	38	92Ho09
18590.1(17)	Penning trap MS	1993	39	93Va04
18591(3)	Beta spectrometry	1993	40	93Ba08
18597(5)	Beta spectrometry	1993	41	93Su32
18589(2)	Beta spectrometry	1995	42	95St26
18597(14)	Beta spectrometry	1995	43	95H114
18591(3) [b]	Beta spectrometry	1995	44	95Lo** [a]
Average weighting ± [tS or MBAYS]	18590.6+1.1 eV σ_{min}=1.7 eV			
Recommended value	18591(2) eV			

a   NSR figure not found.
b   Calculated by the evaluator.

The original results in Table 2.4 for measurements using beta spectrometry have been corrected for the spectra of final states, using the analysis by Kaplan, et al. [45]. The Si(Li) measurements have been corrected for the chemical shift +10(3) eV, evaluated by Redondo and Robertson [46].

The weighted mean of all 23 results is equal to 18590.6(7) eV with $X^2=61$ (reduced $X^2/(n-1)=2.8$). This is not too great a deviation in the results, as the tabulated $\left(X^2\right)_{22}^{0.05}$ is equal to 34. In order to obtain the total error of the evaluated value taking into account the independence of the measurements [22-44], it is possible to use the [WM, tS] [18] or [MBAYS] [19] methods of statistical data treatment: $Q'_{\beta^-}=18590.6+1.1$ eV ($\sigma_{min}=1.7$ eV). However, considering the uncertainty of the error associated with correction for the spectra of final states [45], and the absence in the vast majority of cited results of measurements of decimal fractions of eV, we give the recommended value of Q_{β^-} as 18591(2) eV.

2.4.3. Beta spectrum boundary energy of tritium (E^o)

The beta spectrum boundary energy of tritium depends on the chemical composition of the tritium in the experiment. The expression for E^0_β of molecular tritium differs from E^0_β of a "bare" nucleus by the energy of the chemical shift $\Delta E=B(RHe+)-B(RT)$ [45, 46] which is calculated taking into account the spectrum of final states (SFS). (Here, the quantities B denote the electron binding energy for an He^+ ion and a tritium atom, and R denotes the chemical composition.)

For the known difference in the atomic mass of ^3He-^3H (ΔMc^2), the beta spectrum boundary energy of tritium, measured in a certain experiment, is equal to:

$$E'^0_\beta = \Delta Mc^2 \ E_{rec} - [B(He)-B(T)] + [B(RHe^+)-B(RT)],$$

where E_{rec} is the recoil energy of a helium ion.

For a tritium atom
$$E^0_\beta = \Delta Mc^2 - 3.4 \text{ eV} - 64.3 \text{ eV}$$

where $\Delta E=40.82$ eV. Using the recommended value for Mc^2, the beta spectrum boundary energy of the tritium nuclide is obtained in this way as 18564 eV. It is difficult to evaluate the error in the calculation of ΔE [45]. Assuming that it is approximately equal to the evaluated error for ΔMc^2, we obtain $E^0_\beta(^3H$-nuclide)=18.564(3) eV.

For the real chemical forms of tritium sources in beta spectrometry, the boundary energies of beta particles of ^3H differ from the atomic value. For the molecular forms of HT, CH_3T and valine, the calculated value of E^0_β amounts to 18572(3) eV, on the assumption

that Q_β=18591(2) eV. The boundary energies E^0_β measured in recent experiments are given below:

87Bo07	valine	18579.4±4 eV
93Ba08	molecular tritium	18574.8±0.6 eV
95Su32	$C_{14}H_{16}TeO_2N_3$	18578.3±5.1 eV
95St26	gaseous tritium	18568.5±2.0 eV
95Lo**	gaseous tritium	18570.5 eV

2.4.4. *Average energy of the beta particles of tritium per disintegration ($<E_\beta>$)*

Table 2.5 shows the available data concerning $<E_\beta>$. The recommended value of $<E_\beta>$ was obtained as a weighted mean after corrections had been made to the original results of experiments and calculations. The calculation of $<E_\beta>$ for the recommended value Q_β=18.591(2) keV with the LOGFT program used in ENSDF evaluations, results in a value of 5.68(10) keV [55].

Table 2.5.: Available data on the average energy of beta particles of tritium per disintegration

Reference		Method	Published value (keV)	Corrected value (keV)	Adopted value (keV)
No.	NSR figure				
4	50Je60	Calorimetry	5.69(4)	1 5.69(4)[a]	5.68(4)
47	58Gr93	Calorimetry	5.57(1)	5.68(2)[c]	5.68(2)
48	61Pi01	Calorimetry	5.73(3)	5.68(3)[b]	5.68(3)
49	72Ma72	Calculation	5.		5.7(1)[e]
50	85Ma**	Calculation	5.684(5)	5.680(5)[d]	5.68(1)
51	85Ga**	TDCR*)	5.70		5.70(2)[e]
52	87La**	Calculation	5.71(3)	5.70(3)[d]	5.70(3)
Recommended value			5.68(1) keV		

a   Corrected for the adopted $T_{1/2}(^3H)$=12.32(2) years and a thermal output of 0.324(1) W/year.
b   Corrected for the adopted $T_{1/2}(^3H)$=12.32(2) years.
c   Corrected for the adopted $T_{1/2}(^3H)$=12.32(2) years and a thermal output 0.324(1) W/year.
d   Corrected for the recommended value of the decay energy (Q_β = 18.5906 keV).
e   Error adopted by the evaluator.
*)   See also 94Si21 [53].

2.5. REFERENCES

[1] O'NEAL, R.D., GOLDHABER, M., Phys. Rev. 58 (1940) 574.

[2] GOLDHABER, M., ROBINSON, E.S., SPENCE, R.W., Phys. Rev. 72 (1974) 973.

[3] NOVICK, A., Phys. Rev. 72 (1947) 972.

[4] JENKS, G.H., SWEETON, F.H., GHORMLEY, J.A., Phys. Rev. 80 (1950) 990.

[5] JONES,W.M., Phys. Rev. 83 (1951) 537.

[6] JONES, W.M., Phys. Rev. 100 (1955) 124.

[7] POPOV, M.M., et al., Atomnaya ehnergiya 4 (1958) 269; J. Nuclear Energy 9 (1959) 190.

[8] MERRITT, J.S., TAYLOR, J.G.V., Chalk River Report AECL-2510 (1966).

[9] JORDAN, K.C., BLANKE, B.C., DUDLAY, W.A., J. Inorganic Nuclear Chemistry 29 (1967) 2129.

[10] JONES, P.M.S., J. Nucl. Mater. 21 (1967) 239.

[11] RUDY, C.R., JORDAN, K.C., Tritium Half-Life. MLM-2458, Monsanto Research Corporation, Miamisburg, Ohio.

[12] UNTERWEGER, M.P., et al., Intern. J. Appl. Rad. Isotopes 31 (1980) 611.

[13] BUDICK, B., HONG LIN, Bull. Amer. Phys. Soc. 32 (1987) 1063.

[14] OLIVER, B.M., et al., Intern. J. Appl. Rad. Isotopes 38 (1987) 959.

[15] SIMPSON, J.J., Phys. Rev. 035 (1987) 752.

[16] OLIVER, B.M., BRETSCHER, M.M., FARRAR, H. IV, Intern. J. Appl. Rad. Isotopes 40 (1989) 199.

[17] BUDICK, B., JIANSHENG CHEN, HONG LIN, Phys. Rev. Lett. 67 (1991) 2630.

[18] CHECHEV, V.B., Voprosy Atomnoj Nauki i Tekniki, 1997, TIYAS-KHT, Special Edition, P. 149 [in Russian].

[19] KAFALA, S.F., MACMAHON, T.D., GRAY, P.W., Nucl. Instrum. Method Phys. Res. A339 (1994) 151.

[20] HOLDEN, N.E., Pure and Applied Chemistry 62 (1990) 941.

[21] AUDI, G., WAPSTRA, A.H., Nucl. Phys. A565 (1993) 1; ibid. A595 (1995) 409.

[22] SMITH, L.G., WAPSTRA, A.H., Phys. Rev. C11 (1975) 1392.

[23] SMITH, L.G., KOETS, E., WAPSTRA, A.H., Phys. Lett. 102Bf (1981) 114.

[24] DEBRIN, A.V., ROREKO, L.A., Yadernaya Fizika 38 (1983) 1105.

[25] NIKOLAEV, E.N., et al., Pis'ma v Zh. Ehks. Teor. Fiz. 39 (1984) 441; (JETP Lett.) 39 (1984) 534.

[26] LIPPMAA, E., et al., Phys. Rev. Lett. 54 (1985) 285.

[27] TALROSE, V.L., NIKOLAEV, E.N., Phys. Rev. Lett. Advances in Mass-spectrometry 1985 (Wiley, New York, 1985) 343.

[28] SIMPSON, J.J., DIXON, W.R., STOREY, R.S., Phys. Rev. C3K (1985) 1891.

[29] GORSHKOV, M.V., et al., Metrologiya 8 (1986) 10.

[30] FRITSCHI, M., et al., Phys. Rev. Lett. 173B (1986) 485.

[31] BORIS, S.D., et al., Phys. Rev. Lett 58 (1987) 2019; Pis'ma v Zh. Ehks. Teor. Fiz. 45 (1987) 267 (JETP Lett. 45 (1987) 333).

[32] KAWAKAMI, H., et al., Phys. Lett. B187 (1987) 198.

[33] BRUDANIN, V.B., et al., Preprint Ob"ed. Inst. Yad Issled. (Jt Inst. Nucl. Res) P6 (1988) 936 [in Russian].

[34] STAGGS, S.T., et al., Phys. Rev. 039 (1989) 1503.

[35] BUDICK, B., CHEN, J., LIN, H., Phys. Rev. Lett. 67 (1991) 2626.

[36] ROBERTSON, R.G.N., et al., Phys. Rev. Lett. 67 (1991) 957.

[37] KAWAKAMI, H., et al., Phys. Lett. 67 (1991) 105.

[38] HOIZSCHUH, E., FRITSCHI, M., KUNDIG, W., Phys. Lett. 287B (1992) 381.

[39] VAN DYCK, R.S., FARNHAM, D.L. Jr., SCHWINBERG, P.B., Phys. Rev. Lett. 70 (1993) 2888.

[40] BACKE, H., et al., Nucl. Phys. A553 (1993) 313.

[41] HANCHENG, SUN, et al., Chinese J. Nucl. Phys. 15 (1993) 261.

[42] STOEFFI, W., DECRNAN, D.J., Phys. Rev. Lett. 75 (1995) 3237.

[43] HLDDEMANN, K.H. Yr., DANIEL, H., SCHWENTKER, O., J. Phys. (London) 621 (1995) 639.

[44] LOBASHEV, V.M., Proc. IV Int. Symp. on Weak and Electromagnetic Interaction in Nuclei, Osaka, Japan, 12-16 June 1995, Singapore, WS (1995) 165; see also BELESEV, A.I., et al., Phys. Lett. B350 (1995) 263.

[45] KAPLAN, I.G., SMELOV, G.V., SMUTNY, V.N., Phys. Lett. 1618 (1985) 389.

[46] REDONDO, A., ROBERTSON, R.G.H., Phys. Rev. 040 (1989) 368.

[47] GREGORY, D.P., LANDSMAN, D.A., Phys. Rev. 109 (1958) 2091.

[48] PILLINGER, W.L., HENTGES, J.J., BLIER, J.A., Phys. Rev. 121 (1961) 232.

[49] MANTEL, J., Intern. J. Appl. Rad. Isotopes 23 (1972) 407. In: A handbook of radioactivity measurement procedures.

[50] MARTIN, M.J., NCRP Report No. 58 (1985), 2nd Edition, NCRP, Bethesda, Maryland, 368-373, see [54].

[51] GARSIA-TORANO, E., GRAU MALONDA, A., Comp. Phys. Commun. 36 (1985) 307, see [53].

[52] LAGOUTINE, F., COURSOL, N., LEGRAND, J., Table of Radionuclides, ISBN-2-7272-0078-1 (LMR), (1982-1987) [in French].

[53] SIMPSON, B.R.S., MEYER, B.R., Nucl. Instrum. Methods Phys. Res. A339 (1994) 14.

[54] GENKA, T., KOBAYASHI, K, HAGIWARA, S., Intern. J. Appl. Rad. Isotopes 38 (1987) 845.

[55] BE, M.M, Priv. Comm. (1998).

3. Evaluation of the data for ^{36}Cl

The results of the evaluation of nuclear and atomic data for the radionuclide ^{36}Cl using information published up to 1998 are given below. In contrast to ^{3}H, the amount of new published data for ^{36}Cl is quite small and the evaluated values of the characteristics have changed little in comparison with the reference data of 1980 and 1990.[*]

3.1. *Decay scheme*

98.1% of ^{36}Cl is converted by β^{-} decay to the ground state of ^{36}Ar, 1.9% is converted by electron capture, and 0.0017% is converted by β^{+} decay to the fundamental state of ^{36}S.
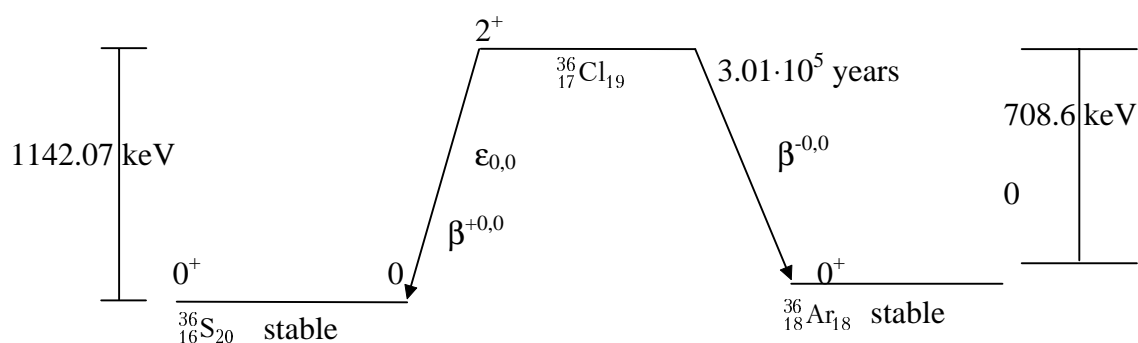
3.2. *Nuclear data*

$T_{1/2}$:   3.01(3)·10^{5} years
Q_{β}-: 708.6(3) keV
Q_{ε}: 1142.07(25) keV

3.2.1. *β-transition*

	Energy, keV	Probability P^{-}	Nature	lg ft.
β$^{-0,0}$	708.6(3)	0.981(1)	Non-unique second-order forbidden	3.05

---

[*]   Khol'nov, Yu.V., Chechev, V.P., Kamynov, Sh.V., Kuz'menko, N.K., Nedovesov, V.G., Characteristics of the radiation of radionuclides used in the national economy. Evaluated data. Handbook. Moscow, Atomizdat, 1980;

Chechev, V.P., Chukreev, F.E., Decay and radiation characteristics of long-lived radionuclides used in the economy and in scientific research. (Evaluated data), Handbook. I.V. Kurchatov Institute of Atomic Energy (1990).

3.2.2. *Electron capture transition*

	Energy keV	Probability P_{ec}	Nature	lg ft	P_k	P_L	P_M^+
$\varepsilon_{o,o}$	1142.07(25)	0.019(1)	Non-unique second- order forbidden	13.5	0.901(7)	0.089(7)	0,010(1)

3.2.3. β^+-*transition*

	Energy, keV	Probability P_β^+	Nature	lg ft
$\beta^{+0,0}$	120.07(25)	$1.5(3)\cdot 10^{-5}$	Non-unique second-order forbidden	14,5

3.3. Atomic data

S, Z = 16 ω_K 0.0804(19)
　　　　　　　　nKL 1.807(5)
Ar, Z = 18 ω_K 0.120(3)
　　　　　　　　nKL 1.697(6)

3.3.1. *X-radiation*

		Energy, keV	Relative probability
S	XK	2.3066-2.464	
	$K\alpha_2$	2.3066	0.505(3)
	$K\alpha_1$	2.3078	1
	$K\beta$	2.457-2.464	0.093(6)
Ar	X_K	2.9453-3.190	
	$K\alpha_2$	2.9453	0.505(3)
	$K\alpha_1$	2.9574	1
	$K\beta$	3.177-3.190	0.162(5)

3.3.2. *Auger electrons*

		Energy, keV	Relative probability
S	eAK	1.98-2.46	
	KLL	1.98-2.12	1
	KLX	2.22-2.30	0.124(8)
	KXY	2.44-2.46	0.0039(5)
Ar	eAK	2.51-3.17	
	KLL	2.51-2.60	1
	KLX	2.83-2.93	0.216(7)
	KXY	3.14-3.17	0.0116(7)

3.4. Radiation emission

3.4.1. Electron radiation

		Energy, keV	Number of electrons per 100 disintegrations
	β^-	0-1142	98.1(1)
S	eAK	1.98-2.46	1.57(10)
	KLL	1.98-2.12	1.40(9)
	KLX	2.22-2.30	0.17(2)
	KXY	2.44-2.46	0.005(1)
Ar	eAK [*]	2.51-3.17	0.130(19)
	KLL	2.51-2.60	0.106(16)
	KLX	2.83-2.93	0.023(4)
	KXY	3.14-3.17	0.0012(2)

[*]   Emission of Auger electrons of Ar is associated with the autoionization of the K-shell accompanying the β^- decay of ^{36}Cl.

3.4.2. Photon radiation

		Energy, keV	Number of photons per 100 disintegrations
S	XK	2.3066-2.464	0.38(8)
	$K\alpha_2$	2.3066	0.044(3)
	$K\alpha_1$	2.3078	0.086(5)
	$K\beta$	2.457-2.464	0.0080(7)
Ar	XK [*]	2.9453-3.190	0.0205(30)
	$K\alpha_2$	2.9453	0.0062(10)
	$K\alpha_1$	2.9574	0.0123(19)
	$K\beta$	3.177-3.190	0.0020(3)
	γ_a [**]	511.00	0.0030(6)

[*]   *Emission of KX radiation of Ar is associated with autoionization of the K-shell accompanying β^- decay of ^{36}Cl.*

[**]   *Annihilation γ_a radiation occurs in the source from positrons of β^+ decay.*

3.4.3. β^--particles

	Boundary energy, keV	Average energy, keV	Average energy per disintegration, keV $<E_{\beta^-}>$	Number of electrons per 100 disintegrations
β^-	708.6(3)	251.20(11) [*]	246.4(4) [*]	96.1(1)

[*]   Calculated for the allowed form of the β^- spectrum; see Section 3.6.7.

3.4.4. β^+-particles

	Boundary energy, keV	Average energy, keV	Average energy per disintegration, keV $<E_{\beta^+}>$	Number of electrons per 100 disintegrations
β^+	120.07(25)	50.24(10) [*]	0.075(15) [*]	0.0015(3)

[*]   Calculated for the allowed form of the β^+ spectrum; see Section 3.6.7.

3.5. *Basic mode of production* $^{35}C1(n,\gamma)^{36}C1$

3.6. *Substantiation of the evaluated data obtained for the decay characteristics of* $^{36}C1$

3.6.1. *Decay scheme and decay energies*

The decay scheme for ^{36}C1 is based on the measurements in Refs [1, 2]. The decay energies $(Q_{\beta^-}, Q_\varepsilon)$ are taken from Ref. [5]. They are based on many measurements. The references to earlier measurement results (up to 1980) can be found in the handbook [19].

3.6.2. *Half-life*

Measured values of the partial half-life of ^{36}Cl for β^- decay and also ^{36}Ar$(T_{\frac{1}{2}}\beta^-)$ are presented in Table 3.1.

Table 3.1.: Results of the measurements of the half-life of ^{36}Cl for decay of ^{36}Cl$\rightarrow^{36}$Ar

Reference		$T_{\frac{1}{2}}\,\beta^-$	Method
No.	NSR figure	in 10^5 years	
14	47Hu**	20	
15	470v**	10	
16	49Re**	2	
10	49Wu15	4,4(5)	Specific activity β(GM)
11	55Ba93	3,08(3)	Specific activity 4πβ(pc)
12	57Wr37 [a]	2,6(4)	C1(n,γ)-yield, β(GM)
12	57Wr37 [b]	2,5(4)	Specific activity, β(GM)
13	66Go07 [a]	3,10(4)	Specific activity, 4πβ(pc)
13	66Go07 [b]	3,06(2)	Specific activity, liquid scint.

Six results of measurements with stated error [10-13] were selected for statistical data treatment (set "1" = set "2", see description of the evaluation technique in Ref. [17]). In set "2" among the six results the weight of the measurement 66Go07[b] exceeds 0.50 (58.5%). Taking this into account and using the LWM procedure [18], the data set "3" was formed. The final results of the data treatment are shown below.

Table 3.2.: The results of treatment of data for $T_{1/2}$ β^- ^{36}C1, obtained using various statistical procedures

Procedure	Half-life (period) (β^-), in 10^5 years	Error, in 10^5 years
UWM	0.31233E+01	0.27681E+00
WM	0.30732E+01	0.16890E-01
CHV	0.23630E+01	0.13094E+00
UINF	0.30732E+01	0.25392E-01
PINF	0.30732E+01	0.25392E-01
BAYS	0.30732E+01	0.32781E-01
MBAY8	0.30732E+01	0.28389E-01
LWM	0.30732E+01	0.25392E-01
lEXW	0.30647E+01	0.24180E+00
NORM	0.30729E+01	0.18892E-01
RAJ	0.30722E+01	0.18897E-01
WM, tS	0.30732E+01	0.27931E-01
Recommended value	$3.07(3) \cdot 10^5$ years	

The weighted mean with error tS was chosen as the recommended value:

$$T_{1/2_\beta}\text{-}(^{36}C1) = (3.07 \pm 0.03) \cdot 10^5 \text{ years}$$

Hence, the **total** half-life of ^{36}C1 is obtained as

$$T_{1/2_\beta}\text{-} \times 0.981(1) = 3.01(3) \cdot 10^5 \text{ years}$$

3.6.3. Electron capture

The recommended values of P_K, P_L and P_M were calculated using the ratio $P_L/P_K=0.099(8)$, which was obtained as the weighted mean of the theoretical value $(P_L/P_K)_T=0.094(5)$ and the experimental value $(P_L/P_K)_{exp}=0.112(8)$, measured in Ref. [8]. The theoretical value $(P_L/P_K)_T$ was obtained from the tables in Ref. [6] and with the aid of the LOGFT program on the assumption of an allowed transition, using the Q_ε value and taking into account the error of using P_K and P_L for the allowed transition instead of the unknown P_K and P_L for the non-unique second-order forbidden transition of ^{36}C1$\rightarrow$^{36}S (0.0). According to Ref. [20] the error from using P_K and P_L tabulated in Ref. [20] is no more than 3% for such transitions, if Q is much greater than the electron binding energy on the K-shell and the nuclear charge is small. For the purposes of comparison, note that calculation of P_L/P_K for the allowed transition with the LOGFT program gives 0.0944 in agreement with the tables of Ref. [6]. For the relative error $(P_L/P_K)_T$, we have taken a conservative estimate of 5%, considering the nature of the transition $\varepsilon_{0.0}$ (second-order forbidden). The error of the

recommended (weighted mean) value P_L/P_K=0.099(8) was obtained in accordance with the evaluation procedure in Ref. [17] as the scattering error S=0.008.

The ratio P_{M+}/P_K=0.0115(12) was taken from the tabular values of P_{M+}, P_K for allowed transitions with an error of 10%.

The probability of electron capture P_{EC}=0.019(1) was calculated, using the measured ratio $P\varepsilon_K/P_{\beta-}$=0.017(1) [1].

3.6.4. β^+-transitions

The probability $P_{\beta+}$=1.5(3)$\cdot10^{-5}$ as obtained by averaging the experimental data presented in Table 3.3.

The recommended value was obtained as the weighted mean using the LWM-procedure (see [17, 18]), which involved reducing the weight of the result of the measurement 67Pi03 up to 50% prior to the final averaging.

3.6.5. β^--transition

The probability $P_{\beta-}$=0.981(1) was calculated using the balance equation $P_{\beta-}$=1-P_{EC}-$P_{\beta+}$.

3.6.6. Atomic data

The atomic constants ω_K, n_{KL} were taken from Ref. [7]. The X-radiation energies were calculated from the wavelengths (in Å) given in Ref. [9]. The Auger electron energies were taken from Ref. [4].

The relative probabilities of the emission of components of KX-radiation and K-Auger electrons were taken from the tables in Ref. [7].

3.6.7. Radiation characteristics

The probabilities of emission of K-Auger electrons and components of KX-radiation from sulphur were calculated from the probability of electron capture P_{EC} and the adopted values of P_K and ω_K.

The probabilities of emission of K-Auger electrons and components of KX-radiation from argon were calculated from the ratio $P_{XK}(Ar)/P_{XK}(S)$=0.149(22) found in Ref. [3], and the atomic data in Section 3.3.

The number of photons per 100 disintegrations for annihilation radiation was calculated as $2I_{\beta+}$ where $I_{\beta+}$ is the number of β^+ decay positrons per 100 disintegrations.

The β^- spectrum boundary energy for ^{36}Cl was obtained from the relation $E_{\beta-} = Q_{\beta-} -E_{rn}$, where E_{rn} is the recoil nucleus energy. The β^+-spectrum boundary energy for ^{36}Cl was calculated as $E_{\beta+} = Q_\varepsilon -E_{rn} - 1022.00$ keV. The average energies of the $\beta^\pm$-spectra, calculated using the data in the tables of Ref. [20] and the LOGFT program on the assumption of an

allowed form are not the actual average $\beta^{\pm}$-particle energies, since $\beta^{\pm}$-transitions of ^{36}C1 are related to non-unique forbidden transitions with the spin variation $4I=2$. The nuclear matrix elements for the probabilities of these transitions are not known. Mantel has [23] calculated the average energy of the β^--spectrum for ^{36}C1 as 320 keV, assuming the spectrum to be close to the unique first-order forbidden form. This value is significantly higher than the one given in Section 3.4.3 for the allowed form of the beta-spectrum.

Table 3.3.:Results of the measurement of the probability of β^+ decay of ^{36}C1 ($P_\beta+$)

Reference		P^+ (x 10^5) (Set "1" = "2")	P^+ (x 10^5) (Set "3")
No.	NSR figure		
8	62Do07	1.2(5)	1.2(5)
21	62Be29, 63Be38	2.3(9)	2.3(9)
22	65To**	1(1)*)	1(1)
2	67Pi03	1.06(11)	1.60(40)
Recommended value		1,5(3)	

*)   Error assigned by the evaluator.

REFERENCES

[1]   DREVER R.W.P. AND MOLJK A., Phil.Mag. 46(1955)1337.
[2]   PIERSON W.R., Phys.Rev. 159(1967)953.
[3]   LJUBICIC A., JURCEVICIC M., VLATKOVIC M., LOGAN V.A., Phys.Rev. 013(1976)881.
[4]   LARKINS F.P., ADNDT 20(1977)313.
[5]   AUDI G. AND WAPSTRA A.N., Nucl.Phys. A595(1995)409.
[6]   SCHONFELD E., Report PTB-6.33-95-2 (1995).
[7]   SCHONFELD E. AND JANBEN H., Nucl.lnstr.Meth. Phys.Res. A369(1996)527.
[8]   DOUGAN P.W. et al., Phil.Mag.. 7(1962)1223.
[9]   BEARDEN J.A. Rev.Mod.Phys. 39(1967)78.
[10]   WU, C.S., TOWNES, C.N., AND FEIDMAN L., Phys.Rev. 76(1949)962.
[11]   BARTHOLOMEW P.M. et al., Can.J.Phys. 33(1955)43.
[12]   WRIGHT H.W. et al., Nucl.Sci.Eng. 2(1957)427.
[13]   GOLDSTEIN G., INORG J. Nucl.Chem. 28(1966)937.
[14]   HUGHES D.J., EGGLER C., AND GOLDSTEIN G., U.S. Atomic Energy Comm.Rept. CP-3801 (1947).See also [11].
[15]   OVERMAN R.T., U.S. Atomic Energy Comm.Rept. AECD-875 (1947). See also [11].
[16]   REYNOLDS S.A., U.S. Atomic Energy Comm.Rept. ORNL-286 (1949). .See also [11].
[17]   CHECHEV V.P.. In: Proceedings of the international Symposium "Advances in α-, β- and γ-Ray Spectrometry", Pushkin (Petersburg, Russia), September, 1996. CIEMAT, 28040-Madrid (1997)87.
[18]   KAFALA S.F., MACMAHON T.D., GRAY P.W., Nucl. Instrum.Methods Phys.Res.

A339(1994)151.

[19] KHOL'NOV, Yu.V., CHECHEV, V.P., KAMYNOV, Sh.V., KUZ'MENKO, N.K., NEDOVESOV, V.G., Characteristics of the radiation of radionuclides used in the national economy. Evaluated Data. Handbook. Moscow Atomizdat (1980) [in Russian].

[20] DZHELEPOV, V.S., ZYRYANOVA, L.N., SUSLOV, Yu.P., Beta processes, Nauka

[21] Berenyi D., Phys.Lett. 2(1962)332; Acta Phys.Acad.Sci.Hungary 16(1963)101; Fiz.SzemIe 16(1966)21. .See also [2].

[22] Tolbert W.R. et al., Bull.Amer.Phys.Soc. 10(1965)589. See also [2].

[23] Mantel J., Intern.J.AppI.Pad. Isot. 23(1972)407.

VALIDATION OF THE ABBN/CONSYST CONSTANTS SYSTEM.

PART 1: VALIDATION THROUGH THE CRITICAL EXPERIMENTS ON COMPACT METALLIC CORES

T.T. Ivanova, G.N. Manturov, M.N. Nikolaev, E.V. Rozhikhin,

M.Yu. Semenov, A.M. Tsiboulia,

State Scientific Centre of the Russian Federation - Institute for Physics and
Power Engineering, Obninsk

VALIDATION OF THE ABBN/CONSYST CONSTANTS SYSTEM. Part 1:
Validation through the Critical Experiments on Compact Metallic Cores. World-
wide compilation of criticality safety benchmark experiments, evaluated due to an
activity of the International Criticality Safety Benchmark Evaluation Project
(ICSBEP), discovers new possibilities for validation of the ABBN-93.1 cross
section library for criticality safety analysis. Results of calculations of small
assemblies with metal-fuelled cores are presented in this paper. It is concluded that
ABBN-93.1 predicts criticality of such systems with required accuracy.

Introduction

The ABBN/CONSYST constants system includes the ABBN-93 constants set and the
CONSYST program which prepares these constants for calculations using recommended
algorithms. They were certified as recommended data in 1995 by the State Information
Service for Standard Reference Data (certificate No. 444, dated 1 August 1995). Unlike
earlier versions of the ABBN constants, the ABBN/CONSYST constants system is
recommended not only for fast power reactor calculations, but also for calculations for
thermal neutron and intermediate neutron reactors, radiation shield, and criticality safety of
the external fuel cycle, for calculating the radio-nuclide composition of spent fuel and
irradiated materials, and for evaluating radiation damage to materials, etc.   This
recommendation was based on a thorough verification report [2] which was subjected to

expert assessment by experienced specialists representing various fields and specialities in the nuclear power development area. In the interim, however, a large quantity of additional experimental data has become available, chiefly thanks to the activities of the International Critical Safety Benchmark Experiment Project (ICSBEP). Pursuant to these activities, the International Handbook of Evaluated Criticality Safety Benchmark Experiments [3] was issued (subsequently referred to as the Handbook) which contains detailed descriptions of carefully evaluated critical experiments performed in various countries. Russia too has made a major contribution to the Handbook.

The series of publications of which this article forms the first is devoted to a validation of the ABBN/CONSYST constants system through the experimental results collated in the above-mentioned Handbook. The main stimulus for this work was the need to validate the programs and databases used to evaluate nuclear safety in the external fuel cycle for the purposes of their subsequent licensing by Gosatomnadzor [Federal Nuclear and Radiation Safety Authority of Russia]. However, since nuclear safety calculations are performed using programs which solve the strict transport equation with a detailed description of the geometry (Monte Carlo method), many of the benchmark experiments used to validate criticality safety evaluation programs can also be used as benchmarks to validate constants' software. Such experiments include, in particular, critical experiments on compact cores carried out within the framework of nuclear weapons development programmes in the USA and Russia. A computational analysis of these experiments is given in this article. The calculations were carried out using the KENO-Va and KENO-VI codes employing the 299-group ABBN-93 constants (the version transmitted to the RSICC). For comparison, the results of calculations carried out using the MCNP program are also given with a detailed description of the energy dependence of the cross-sections based on the ENDF/B-V evaluated nuclear data library (computational instrument licensed in the USA for criticality safety calculations). The calculation results for foreign constants we took from the relevant foreign sources.

1. Critical assemblies with no reflector with an enriched uranium core

The results of a comparison of the calculated data with the experimental data are given below. The differences between the calculated value $(k_{c,i})$ and the experimental value $(k_{e,i})$ of the multiplication coefficient are shown as a percentage. The results generated by the CONSYST-KENO package are given, together with the error levels obtained in the evaluation of the experimental data which are given in the descriptions of the evaluations (see Ref. [3]). The experimental error levels $(\delta k_{e,i})$ are also shown as percentages with a "±" sign. Next, the statistical error level $(\delta k_{c,i})$ is given for the calculation result using the Monte Carlo method. This is shown in brackets and is expressed as a whole number of hundredths of a per cent. Thus, the value 0.36±0.16(7) means that the difference between the calculated and experimental values of k_{eff} is 0.36%, the error level of the experimental value is 0.16%, and the statistical error level of the calculation is 0.07%. Thus, the error level of the difference is

$$\delta k_i = \sqrt{\delta k_{e,i}^2 + \delta k_{c,i}^2} = \sqrt{0.16^2 + 0.07^2} = 0.175.$$

The results obtained using the MCNP program and the ENDF/B-V constants are also taken from Ref. [3] for American critical assemblies, and from Ref. [4] for Russian critical

assemblies. The latter source also gives the data obtained using the ENDF/B-VI library. These are also shown in the table. For the results obtained using the MCNP program, only the statistical error level is given; the experimental error level is not duplicated.

For an overall evaluation of the divergence between the calculation and the experiment, the following mean characteristics need to be calculated.

The expected root-mean-square spread of the divergence between the calculation and the experiment determined from the evaluated error levels of both:

$$\delta k_{exp} = \sqrt{\frac{n}{\sum_{i=1}^{n} 1/\delta k_i^2}} \, .$$

The mean deviation of the calculation from the experiment:

$$\Delta k = \frac{\sum_{i=1}^{n} (k_{c,i} - k_{e,i})/\delta k_i^2}{\sum_{i=1}^{n} 1/\delta k_i^2} \, .$$

The observed root-mean-square spread of the divergence of the experimental data (root-mean-square deviation from the results of the calculation performed using the constants which yield the best match with the experimental data, i.e. $\Delta k = 0$):

$$\delta k_{cal} = \sqrt{\frac{\sum_{i=1}^{n} (k_{c,i} - k_{e,i} - \Delta k)^2/\delta k_i^2}{\sum_{i=1}^{n} 1/\delta k_i^2}} \, .$$

These formulae do not take into account possible correlations between the error levels of the various experiments.

These data show that the calculations using the ABBN-93 and ENDF/B-V constants underestimate k_{eff} by a quarter of a per cent. This underestimation is systematic and is almost twice the error level of each individual experiment. The exception is the assembly with 36% enriched uranium where the calculated value of k_{eff} is slightly higher than the experimental value.

If we exclude this assembly, which differs significantly from the remaining assemblies in both composition and neutron spectrum, the mean divergence increases to -0.29%, and the root-mean-square spread of the experimental data decreases to the level which would be expected working from the evaluated experimental error levels (the contribution of the

statistical error levels of the calculated results is also taken into account, but it is not very significant). The results obtained by averaging for the six assemblies with high-enriched uranium are given in Table 1 in brackets. In this case too, the results obtained using the ABBN-93 and ENDF/B-V constants are practically identical. ENDF/B-VI yields a significantly larger divergence between the experimental and calculated data, but even here the root-mean-square spread calculated after correction for shifting of the calculated values relative to the experimental values is as would be expected from the evaluated experimental error levels.

Table 1. Uranium assemblies with no reflector

Experiment index from the Handbook	Location carried out	Experiment configuration	$(k_c$-$k_e)$ in %, KENO ABBN-93	$(k_c$-$k_e)$ in %, MCNP ENDF/B-V	$(k_c$-$k_e)$ in %, MCNP ENDF/B-VI
IEU-MET-FAST-003	VNIIEF[1]	Sphere (36%)	+0.08±0.17(7)	+0.54(6)	+0.09(9)
HEU-MET-FAST-018	VNIIEF	Sphere (90%)	−0.14±0.14(7)	−0.16(5)	−0.37(6)
HEU-MET-FAST-008	VNIITF[2]	Sphere (90%)	−0.36±0.16(7)	−0.55(6)	−0.64(6)
HEU-MET-FAST-001	LANL	Sphere (94%) (Godiva)	−0.02±0.10(7)	−0.32(9)	
HEU-MET-FAST-007-01	ORNL	Parallelepiped (94%) 25x25x4 cm	−0.49±0.10(8)	−0.30(13)	
HEU-MET-FAST-007-019	ORNL	Parallelepiped (94%) 13x25x6 cm	−0.25±0.10(7)	−0.12(14)	
HEU-MET-FAST-015	VNIITF	Cylinder (96%)	−0.64±0.17(7)	−0.45(6)	−0.73(6)
Expected root-mean-square spread (δk_{exp})			±0.14	±0.14	±0.17
Observed mean divergence ($\Delta k \pm \delta k_{cal}$)			−0.25±0.22 −0.29±0.17*	−0.22±0.26 −0.29±0.14*	−0.43±0.52 −0.56±0.16*

* Values obtained without taking into account the data for the sphere of 36% enriched uranium.

From the above we may conclude that the set of experimental data obtained for the six assemblies with high-enriched uranium with no reflector at the four different institutes is internally consistent and indicates that calculations using the ABBN-93 constants (and the ENDF/B-VI constants) underestimate k_{eff} for such assemblies by almost 0.3%. In future this

---

[1] All-Russian Research Institute of Experimental Physics
[2] Russian Federal Nuclear Center Institute of Theoretical Physics

divergence could be eliminated by correcting the constants, which would reduce the expected error level of the calculated prediction of the criticality of such systems to less than one tenth of a per cent.

2. Critical spheres made of plutonium with no reflector

Table 2 gives the calculation results for four critical assemblies with plutonium spheres with no reflector. The experiments were carried out at two different institutes. Two assemblies had a high plutonium-240 content (12% and 20%). The last rows of the table give the same mean characteristics as for the uranium critical assemblies.

As may be seen from the above data, the criticality of the plutonium spheres is underestimated in the calculations almost to a greater extent than the criticality of the uranium spheres. The calculations using ABBN-93 underestimate k_{eff} by 0.3%, those using ENDF/B-V by 0.4%, and those using ENDF/B-VI by 0.5%. All these shifts exceed the experimental error levels where evaluated values - judging from the root-mean-square spread of the experimental data - are certainly not overestimated (since the number of experiments is small - a total of 4, the fact that the root-mean-square spread is significantly smaller than the evaluated experimental error levels is no justification for asserting that the evaluated error levels are unjustifiably high). No correlation was found between the divergence and the plutonium-240 concentration.

Table 2.   Plutonium assemblies with no reflector

Experiment index from the Handbook	Location carried out	Experiment configuration	$(k_c - k_e)$ in %, KENO ABBN-93	$(k_c - k_e)$ in %, MCNP ENDF/B-V	$(k_c - k_e)$ in %, MCNP ENDF/B-VI
PU-MET-FAST-022	VNIIEF	(2% ^{240}Pu)	-0.27±0.21(9)	–0.35(5)	–0.41(6)
PU-MET-FAST-001	LANL	(5% ^{240}Pu) Jezebel	-0.21±0.20(6)	–0.43(12)	
PU-MET-FAST-029	VNIIEF	(12% ^{240}Pu)	-0.53±0.20(6)	–0.56(5)	–0.57(6)
PU-MET-FAST-002	LANL	(20% ^{240}Pu) Dirty Jezebel	-0.22±0.20(9)	–0.15(14)	
Expected root-mean-square spread (δk_{exp})			±0.21	±0.22	±0.21
Observed mean divergence ($\Delta k \pm \delta k_{cal}$)			–0.31±0.13	–0.38±0.15	–0.49±0.08

Doubtless a minor correction to the plutonium-239 constants used would bring the calculated data for k_{eff} into line with the experimental data to within the error limits of the latter. Correction of the uranium-235 constants would also bring about a better match between the calculation and the experiment.

3.   Critical spheres made of plutonium in a high-enriched uranium shell

Table 3 gives the results of a comparison of the calculated and experimental data for two critical assemblies with compound cores made of plutonium and uranium. One of them, which was studied at LANL, had a central plutonium core (5% plutonium-240) and a high-enriched (93%) uranium shell 1.7 cm thick; in the other, which was studied at VNIITF, the plutonium core contained 9.3% plutonium-240 and the uranium shell, which was 2.3 cm thick, had an enrichment level of 89.6%.

Clearly, the nature of the divergences between the experimental data and the calculations using the ABBN-93 constants is as was to be expected here, working from the computational analysis of the pure uranium and pure plutonium bare assemblies: the divergence is greater than for the former and less than for the latter. This confirms further the conclusions drawn regarding the underestimation of k_{eff} in the calculations, and the desirability of correcting the constants by fitting the results to the critical experiment data. At the same time it should be noted that the calculations using the ENDF/B-V constants for these assemblies show an unexpectedly high level of agreement with the experiment: the divergences were lower than for both the uranium and the plutonium critical assemblies. However, since there were only two uranium-plutonium assemblies with no reflector this must be viewed as a chance effect. The fact that the root-mean-square spread ($\pm 0.10\%$) is noticeably less than the evaluated experimental error levels and statistical error levels of the calculation ($\pm 0.17\%$) would lead one to expect, despite the fact that these error levels are fairly close to the error levels for the determination of k_{eff} for the uranium ($\pm 0.14\%$) and pure plutonium assemblies ($\pm 0.22\%$), supports this view.

4.   Critical spheres made of uranium-233 with no reflector in an enriched uranium shell

There are a total of three assemblies with metallic uranium-233 in the core. In two of them, the central uranium-233 core is surrounded by a spherical layer of metallic uranium-235 1-2 cm thick. The divergence between the calculation and the experiment for these assemblies are given in Table 4.

Thus, for compact assemblies with uranium-233 the calculations also underestimate k_{eff} by $0.4 \pm 0.2\%$ when using the ABBN-93 constants, and by $0.2 \pm 0.2\%$ when using ENDF/B-V. The $\pm 0.2\%$ error level confirms our opinion that the experimental error levels ascribed to the experimental data, by comparison with the evaluated error levels for the plutonium assemblies and the assemblies with high-enriched uranium, are unjustifiably low. The high root-mean-square spread of the data, by comparison with the calculations using ENDF/B-V, indirectly support this.

Table 3.   Assemblies with a plutonium core with no reflector and a high-enriched uranium shell

Experiment index from the Handbook	Location carried out	Experiment configuration	$(k_c\text{-}k_e)$ in %, KENO ABBN-93	$(k_c\text{-}k_e)$ in %, MCNP ENDF/B-V	$(k_c\text{-}k_e)$ in %, MCNP ENDF/B-VI
MIX-MET-FAST-001	LANL	Pu (5% ^{240}Pu) + 1.7 cm U (93%)	–0.39±0.16(8)	–0.20(8)	
MIX-MET-FAST-003	VNIIEF	Pu (9% ^{240}Pu) + 2.3 cm U (90%)	-0.15±0.16(10)	–0.01(6)	
Expected root-mean-square spread (δk_{exp})			±0.18	±0.17	
Observed mean divergence ($\Delta k \pm \delta k_{cal}$)			–0.28±0.12	–0.09±0.10	

Table 4.   Critical assemblies with a core of uranium-233 with no reflector in an enriched uranium shell

Experiment index from the Handbook	Location carried out	Experiment configuration	$(k_c\text{-}k_e)$ in %, KENO ABBN-93	$(k_c\text{-}k_e)$ in %, MCNP ENDF/B-V	$(k_c\text{-}k_e)$ in %, MCNP ENDF/B-VI
U233-MET-FAST-001	LANL	Sphere of ^{233}U	–0.44±0.10(8)	–0.30(11)	
U233-MET-FAST-002-1	LANL	Sphere of ^{233}U + 1.2 cm ^{235}U	–0.43±0.10(8)	–0.31(9)	
U233-MET-FAST-002-2	LANL	Sphere of ^{233}U + 2.0 cm ^{235}U	–0.28±0.11(8)	+0.07(9)	
Expected root-mean-square spread (δk_{exp})			±0.14	±0.14	
Observed mean divergence ($\Delta k \pm \delta k_{cal}$)			–0.38±0.07	–0.18±0.18	

5.   Uranium and plutonium spheres with a metallic uranium-238 reflector

Table 5 gives the criticality divergences between the calculation and the experiment for assemblies with a metallic uranium reflector and metallic cores of varying composition. All 22 critical states recommended for use as benchmarks for the analysis of programs and constants used for nuclear safety calculations were investigated. The calculated values of k_{eff} for critical assemblies with no reflector were on average persistently lower than the experimental values, but the reverse was found for assemblies with a uranium reflector.

The data show that calculations using both the ABBN-93 constants and the ENDF/B-V constants overestimate the contribution of the uranium reflector to the multiplication coefficient. It should be noted that the energy spectra of the neutrons in the above-mentioned critical assemblies with no reflector containing plutonium and high-enriched uranium are similar to one another, as are the neutron importance spectra. There is therefore every reason to assume that the effect of the reflector on the criticality of both the uranium and plutonium assemblies will be almost identical.

Table 5.   Critical Assemblies with a Metallic Uranium-238 Reflector

Experiment index from the Handbook	Location carried out	Geometry and thickness of reflector	(k_c-k_e) in %, KENO ABBN-93	(k_c-k_e) in %, MCNP ENDF/B-V	(k_c-k_e) in %, MCNP ENDF/B-VI
HEU-MET-FAST-014	VNIITF	Sphere, 4.65 cm	–0.07±0.17(7)	–0.07(6)	–0.31(6)
HEU-MET-FAST-029	VNIIEF	Sphere, 4.70 cm	+0.44±0.20(7)		
HEU-MET-FAST-003-1	LANL	Sphere, 5.08 cm	–0.52±0.50(7)	–0.50(8)	
HEU-MET-FAST-003-2	LANL	Sphere, 7.62 cm	–0.69±0.50(7)	–0.52(9)	
HEU-MET-FAST-003-3	LANL	Sphere,10.16cm	–0.03±0.50(7)	+0.07(11)	
HEU-MET-FAST-003-4	LANL	Sphere, 12.70 cm	–0.18±0.30(7)	–0.13(10)	
HEU-MET-FAST-003-5	LANL	Sphere, 17.78 cm	+0.11±0.30(7)	+0.28(10)	
HEU-MET-FAST-003-6	LANL	Sphere, 20.32 cm	+0.24±0.30(7)	+0.24(11)	
HEU-MET-FAST-003-7	LANL	Sphere, 27.94 cm	+0.30±0.30(7)	+0.41(12)	
HEU-MET-FAST-002-2	LANL	Cylinder, 20 cm	+0.35±0.30(7)	+0.30(10)	
HEU-MET-FAST-002-3	LANL	Parallelepiped, 4x4x3.66", 8"	+0.18±0.30(7)	+0.20(10)	
HEU-MET-FAST-002-4	LANL	Parallelepiped 5x5x2.53", 8"	+0.10±0.30(7)	+0.41(10)	
HEU-MET-FAST-002-5	LANL	Parallelepiped 3x3x7.56",8"	–0.04±0.30(7)	+0.39(10)	
HEU-MET-FAST-002-6	LANL	Parallelepiped 3x3.5x6.0",8"	+0.25±0.30(7)	+0.28(11)	
Expected root-mean-square spread (δk_{exp})			±0.30	±0.32	
Observed mean divergence ($\Delta k \pm \delta k_{cal}$)			+0.11	+0.09	
PU-MET-FAST-010	LANL	Sphere, 4.0 cm	–0.22±0.18(8)	+0.05(9)	
PU-MET-FAST-020	VNIITF	Sphere, 9.65 cm	+0.47±0.17(8)	+0.10(6)	

-26-

Experiment index from the Handbook	Location carried out	Geometry and thickness of reflector	(k_c-k_e) in %, KENO ABBN-93	(k_c-k_e) in %, MCNP ENDF/B-V	(k_c-k_e) in %, MCNP ENDF/B-VI
PU-MET-FAST-006	LANL	Sphere, 20 cm	*+0.06±0.30(8)*	*+0.47(14)*	
Expected root-mean-square spread (δk_{exp})			±0.21	±0.21	
Observed mean divergence ($\Delta k \pm \delta k_{cal}$)			+0.13	+0.14	
MIX-MET-FAST-002-1	LANL	Sphere, 2% ^{240}Pu, 19cm	+0.46±0.42(8)	+0.61(13)	+0.44(13)
MIX-MET-FAST-002-2	VNIITF	Sphere, 5% ^{240}Pu, 19cm	+0.48±0.44(8)	*+0.68(12)*	*+0.68(14)*
MIX-MET-FAST-002-3	LANL	Sphere, 16% ^{240}Pu, 19cm	+0.76±0.48(8)	+0.76(12)	+0.69(11)
Expected root-mean-square spread (δk_{exp})			±0.45	±0.45	±0.45
Observed mean divergence ($\Delta k \pm \delta k_{cal}$)			+0.55	+0.68	+0.67
U233-MET-FAST-003-1	LANL	Sphere of ^{233}U+^{235}U, 2.3cm	−0.31±0.10(8)	+0.03(9)	
U233-MET-FAST-003-2	LANL	Sphere of ^{233}U+^{235}U, 20cm	−0.31±0.11(8)	−0.44(9)	
U233-MET-FAST-006	LANL	Sphere of ^{233}U, 20cm	−0.44±0.14(8)	+0.23(11)	
Expected root-mean-square spread (δk_{exp})			±0.14	±0.14	
Observed mean divergence ($\Delta k \pm \delta k_{cal}$)			-0.34	-0.10	

For convenience, the averaging results from Table 5 and the relevant tables for assemblies with no reflector are summarised below.

Clearly, in all cases the calculated efficiency of the uranium reflector is high, though by an amount which is only a little greater than the error level. In view of the fact that the mean divergences between the calculation and the experiment in the criticality of the uranium and plutonium assemblies differ significantly, it was thought wise - for the purposes of eliminating errors in the computational description of the effect of the reflector on criticality - to cross-compare not the calculated and experimental values of k_{eff} for assemblies with reflectors of varying thickness, but the differences $\delta k_U = k_{eff}$(U-refl.) - k_{eff}(bare). Here the index U indicates the material of the reflector; k_{eff}(U-refl.) is the calculated or, as appropriate, experimental value of the multiplication coefficient for an assembly with a uranium reflector of a specific thickness; k_{eff}(bare) is the corresponding value for an assembly with no reflector with the same core material and studied at the same laboratory. There is a clear reduction in the error levels caused by inaccuracies in the determination of the composition and, in part, the dimensions of the core when determining the experimental differences, and the reflector effect becomes visible in a more or less pure form. Table 6 shows the divergences between

the calculation and the experiment $\Delta k_U = \delta k_{U,c} - \delta k_{U,e}$ together with the experimental and calculation error levels. The last rows of the table give the same mean characteristics as in the preceding tables.

	ABBN-93	ENDF/B-V
Uranium assemblies with a uranium reflector	+0.11±0.30	+0.09±0.30
Uranium assemblies with no reflector	−0.29±0.17	−0.29±0.14
Difference	**+0.40±0.33**	**+0.38±0.33**
Plutonium assemblies with a uranium reflector	*+0.13±0.21*	*+0.14±0.21*
Plutonium assemblies with no reflector	*−0.31±0.20*	*−0.38±0.20*
Difference	***+0.44±0.29***	***+0.52±0.29***
Mixed assemblies with a uranium reflector	+0.55±0.45	+0.68±0.45
Mixed assemblies with no reflector	−0.28±0.20	−0.09±0.20
Difference	**+0.83±0.50**	**+0.77±0.50**
Assemblies containing uranium-233 with a uranium reflector	*−0.34±0.11*	*−0.10±0.11*
Assemblies containing uranium-233 with no reflector	*−0.38±0.11*	*−0.18±0.11*
Difference	***+0.04±0.20***	***+0.08±0.20***

Table 6 gives data only for spherical assemblies. What particular spherical assembly was taken as a basis in each case is indicated in the notes after the table. The descriptions of the evaluations very frequently do not give all the components of the error level ascribable to the experimental value of k_{eff}. Therefore, an accurate evaluation of the error level of the differences between the two experimental values of k_{eff} could only be performed in some cases. In the remaining cases, the error level of k_{eff} for an assembly with a reflector, or of k_{eff} for an assembly with no reflector, was used for the error level of this difference, depending on which of these two values was the greater. As above, the averaging of the unequally accurate results was performed employing a weighting which was inversely proportional to the total dispersion, which is equal to the sum of the squares of the experimental and calculation error levels. In the case of the differences, the contribution of the statistical error levels of the calculated results was often significant.

Table 6.   Effect of a Metallic Uranium-238 Reflector

Experiment index from the Handbook	Location carried out	Reflector thickness	$(\delta k_{U,c}-\delta k_{U,e})$ % KENO ABBN-93	$(\delta k_{U,c}-\delta k_{U,e})$ % MCNP ENDF/B-V	$(\delta k_{U,c}-\delta k_{U,e})$ % MCNP ENDF/B-VI
U233-MET-FAST-003-2 (basis U3MF-001)	LANL	2.3 cm	+0.13±0.10(11)	+0.33(12)	
PU-MET-FAST-010 (basis PMF-001)	LANL	4.0 cm	−0.01±0.20(11)	+0.48(12)	
HEU-MET-FAST-014 (basis HMF-008)	VNIITF	4.65 cm	+0.29±0.17(11)	+0.48(6)	+0.33(6)
HEU-MET-FAST-029 (basis HMF-18)	VNIIEF	4.70 cm	+0.58±0.20(11)		−0.44(6)
HEU-MET-FAST-003-1 (basis HMF-1)	LANL	5.08 cm	−0.50±0.50(10)	−0.18(13)	
U233-MET-FAST-003-2 (basis U3MF-001)	LANL	5.3 cm	+0.13±0.10(11)	−0.14(12)	
HEU-MET-FAST-003-2 (basis HMF-1)	LANL	7.63 cm	−0.67±0.50(10)	−0.20(13)	
HEU-MET-FAST-003-3 (basis HMF-1)	LANL	10.16 cm	−0.01±0.50(10)	+0.39(14)	
HEU-MET-FAST-003-4 (basis HMF-1)	LANL	12.70 cm	−0.16±0.35(10)	+0.19(12)	
HEU-MET-FAST-003-5 (basis HMF-1)	LANL	17.78 cm	+0.13±0.35(10)	+0.60(12)	
MIX-MET-FAST-002 (basis MMF-1)*	LANL	18.9 cm	+0.96±0.40(11)	+0.88(14)	
U233-MET-FAST-006 (basis U3MF-1)	LANL	20 cm	0.00 ±0.14(10)	+0.53(15)	
PU-MET-FAST-006 (basis PMF-001)	LANL	20 cm	+0.27±0.40(11)	+0.90(19)	
HEU-MET-FAST-003-6= HMF-002 (basis HMF-1)	LANL	20.3 cm	+0.26±0.35(10)	+0.56(13)	
HEU-MET-FAST-003-7 (basis HMF-1)	LANL	27.9 cm	+0.32±0.35(10)	+0.73 (15)	
Expected root-mean-square spread (δk_{exp})			±0.25	±0.26	
Observed mean divergence ($\Delta k \pm \delta k_{cal}$)			+0.15±0.25 +0.11±0.38**	+0.33±0.30 +0.40±0.35**	

*   Averaged results for three assemblies containing from 2.3% to 16% plutonium-240 (see text).

**   Averaging results equal weightings given in brackets.

It should be noted that, in a series of cases, clearly not all factors were taken into account in the evaluation of the error levels of the experimental results. Thus, for example, the error level for uranium-233 assemblies with a reflector - according to the description - only takes account of error caused by inaccurate knowledge of the thickness of the reflector. There can be no doubt that the error level of the difference in the experimental values for k_{eff} with a reflector, and with no reflector, is significantly underestimated for all assemblies with uranium-233 in the core. On the other hand, in the description of the evaluation of the HEU-MET-FAST-003 series assemblies, it is noted that the fairly high error level ascribed to k_{eff}

reflects the opinion expressed by the experimenters several years after the experiments were completed. Comparison with the carefully evaluated error levels of other similar experiments leads us to the assumption that the experimenters greatly overestimated the error levels for this experimental series. Therefore, we tried a variant averaging process for the data which assumes that all the results have an identical accuracy level. These data are given in Table 5 in brackets.

Attention is drawn to the following:

1. Irrespective of whether the difference in the evaluated error levels of the experimental results is taken into account in the averaging, or whether all the data are considered to be equally accurate, the mean divergence between the calculated and experimental evaluation of the efficiency of the uranium reflector as shown by the data in Table 5 (0.2-0.3%) is significantly lower than was indicated above by the comparison of the mean divergence between the calculation and the experiment for all assemblies with a reflector and a uranium (or plutonium, or mixed) core and the divergence between the calculation and the experiment for all similar assemblies with no reflector (0.5-0.9%). This definitely indicates that there are correlations in the error levels for the experimental determination of k_{eff} in the same laboratory. When comparing the results with and without a reflector obtained at the same laboratory, the correlated error levels are lower (irrespective of whether the error levels were taken into account in the evaluation or not);

2. The mean divergence between the results of the calculation and the experiment is the same as the evaluated mean error level of an individual experiment and somewhat lower than the root-mean-square spread.

Thus, we may say that the calculated and experimental efficiency of a uranium reflector agree to within error limits (experimental error plays a decisive role). Within error limits, no significant systematic dependence of the divergence between the calculation and the experiment on the thickness of the uranium reflector is observed. This may be clearly seen in Fig.1 where the observed divergence are shown relative to reflector thickness.
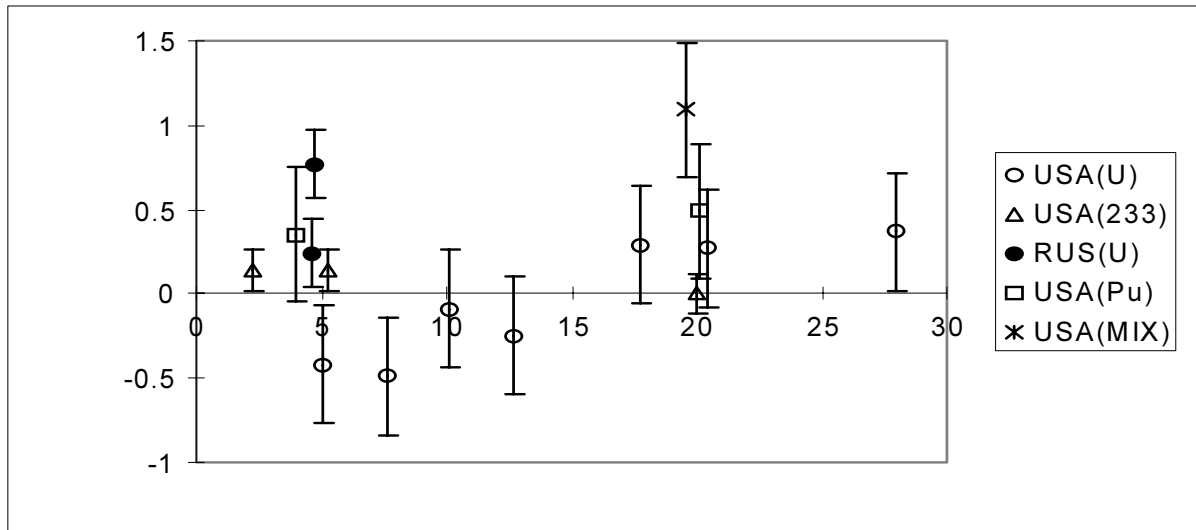
Fig. 1. *Dependence of the divergence (in %% Δk/k) between the calculated and experimental efficiency of a metallic uranium-238 reflector on reflector thickness.*

6. Critical assemblies with reflectors made of polyethylene or water

Nine assemblies of this kind were studied at four different institutes in Russia and the USA. The divergence between the calculation and the experiment for all these assemblies are shown in Table 7.

As we can see, the divergence between the calculated and experimental values for assemblies with polyethylene and water reflectors agree on average with an accuracy approaching the experimental and root-mean-square error levels, which are slightly larger.

Table 8 gives the divergences between the calculation and the experiment for the efficiency of the polyethylene and water reflectors $\Delta k_H = \delta k_{H,c} - \delta k_{H,e}$. These values are determined in exactly the same way as for the uranium reflectors. However, it should be noted that the polyethylene and water reflectors significantly soften the spectrum of the neutrons causing the fission in the core, and it is therefore not at all self-evident that the error levels for the calculated evaluation of the efficiency of these reflectors for both uranium and plutonium assemblies should be identical. Therefore, the mean characteristics of the divergences between the calculation and the experiment are given separately in Table 8 for three uranium and three plutonium assemblies and, finally, for all the spherical assemblies included in the Table. For the uranium assemblies, the ABBN-93 and ENDF/B-V constants can be used to predict the efficiency of the polyethylene reflectors to an accuracy within the expected error levels. The ENDF/B-VI constants yield a slight overestimation (one-and-a-half times the error level) of reflector efficiency. For the plutonium assemblies, only the ENDF/B-V constants describe the efficiency of the polyethylene reflectors to an accuracy within the error levels; the ABBN-93 constants and ENDF/B-VI constants yielded an overestimate of the efficiency three times the expected error level. However, the efficiency of

the thick water reflector when calculated using the ABBN-93 and ENDF/B-V constants for an assembly with a plutonium core was practically identical, and coincided with the experiment within error limits.

Table 7.   Critical assemblies with polyethylene or water reflectors

Experiment index from the Handbook	Location carried out	Geometry; reflector thickness	$(k_c\text{-}k_e)$ in %, KENO ABBN-93	$(k_c\text{-}k_e)$ in %, MCNP ENDF/B-V	$(k_c\text{-}k_e)$ in %, MCNP ENDF/B-VI
HEU-MET-FAST-020	VNIIEF	Sphere; polyethylene 1.45 cm	+0.12±0.28(7)	−0.48(6)	−0.18(7)
HEU-MET-FAST-024	VNIITF	Sphere; steel 0.25 cm + polyethylene 10 cm	−0.62±0.15(8)	−0.40(7)	−0.31(7)
HEU-MET-FAST-011	VNIITF	Sphere; polyethylene 13 cm	−0.06±0.15(8)	−0.49(8)	−0.09(7)
HEU-MET-FAST-007-35	ORNL	Disk; 13x25x2.7 cm + polyethylene 15 cm	−0.61±0.01(8)	−1.26(18)	
PU-MET-FAST-031	VNIIEF	Sphere (10% ^{240}Pu); polyethylene 3.7 cm	+0.29±0.21(9)	−0.07(7)	+0.21(8)
PU-MET-FAST-027	VNIIEF	Sphere (2% ^{240}Pu); polyethylene 5.6 cm	+0.36±0.22(9)	−0.05(7)	+0.28(8)
PU-MET-FAST-024	VNIIEF	Sphere (2% ^{240}Pu); polyethylene 1.6 cm	+0.05±0.20(6)	−0.05(6)	+0.11(6)
HEU-MET-FAST-004	LANL	Sphere with thick water reflector	−0.03±0.15(8)	−0.20(5)	
PU-MET-FAST-011	LANL	Sphere (5% ^{240}Pu) with thick water reflector	−0.37±0.10(9)	−0.07(11)	
Expected root-mean-square spread (δk_{exp})			±0.15	±0.18	±0.20
Observed mean divergence ($\Delta k \pm \delta k_{cal}$)			-0.32±0.33	-0.34±0.23	0.00±0.21

Table 8.　Efficiency of a spherical polyethylene or water reflector

Experiment index from the Handbook	Location carried out	Reflector thickness	$(\delta k_{CH2,c}-\delta k_{CH2,e})$ in %, KENO ABBN-93	$(\delta k_{CH2,c}-\delta k_{CH2,e})$ in %, MCNP ENDF/B-V	$(\delta k_{CH2,c}-\delta k_{CH2,e})$ in %, MCNP ENDF/B-VI
HEU-MET-FAST-020 [basis HMF-018]	VNIIEF	Polyethylene 1.45 cm	+0.26±0.30(12)	–0.32(9)	+0.21(10)
HEU-MET-FAST-024 [basis HMF-008]	VNIITF	Polyethylene 10 cm	–0.36±0.20(11)	+0.15(10)	+0.33(10)
HEU-MET-FAST-011 [basis HMF-008]	VNIITF	Polyethylene 13 cm	+0.30±0.20(11)	+0.06(11)	+0.55(10)
Expected root-mean-square spread for uranium assemblies (δk_{exp})			±0.25	±0.25	±0.24
Observed mean divergence for uranium assemblies ($\Delta k \pm \delta k_{cal}$)			+0.03±0.27	-0.14±0.24	+0.39±0.14
PU-MET-FAST-031 [basis PMF-029]	VNIIEF	Polyethylene 3.7 cm	+0.82±0.20(12)	+0.49(10)	+0.62(11)
PU-MET-FAST-027 [basis PMF-029]	VNIIEF	Polyethylene 5.6 cm	+0.89±0.30(12)	+0.51(10)	+0.69(11)
PU-MET-FAST-024 [basis PMF-022]	VNIIEF	Polyethylene 1.6 cm	+0.32±0.20(6)	+0.30(9)	+0.52(9)
Expected root-mean-square spread for plutonium assemblies (δk_{exp})			±0.24	±0.24	±0.24
Observed mean divergence for plutonium assemblies ($\Delta k \pm \delta k_{cal}$)			+0.61±0.26	+0.42±0.10	+0.60±0.11
HEU-MET-FAST-004 [basis HMF-001]	LANL	Thick layer of H_2O	–0.01±0.17(11)	+0.12(9)	
PU-MET-FAST-011 [basis HMF-001]	LANL	Thick layer of H_2O	–0.16±0.20(11)	+0.36(11)	
Expected root-mean-square spread for all assemblies (δk_{exp})			±0.21	±0.21	±0.24
Observed mean divergence for all assemblies ($\Delta k \pm \delta k_{cal}$)			-0.08±0.07	+0.22±0.12	+0.50±0.24

Thus the whole set of available data hardly provides grounds for asserting that the overestimation of the efficiency of the polyethylene reflector noted above for plutonium assemblies is statistically significant. The mean characteristics of the divergences between the calculation and the experiment for all spherical assemblies, which are given in the last rows of Table 8, show that the mean divergence between the calculation and the experiment using both the ABBN-93 and ENDF/B-V constants does not exceed the root-mean-square spread.

7.   Critical assemblies with iron reflectors

For assemblies with iron reflectors we only have Russian data. The VNIIEF produced data on the criticality of two spherical assemblies with a high-enriched uranium core and four spherical assemblies with a plutonium core. In addition, data are available on the criticality of the BR-1 reactor which has iron shielding (this is a quasi-cylindrical critical system). The divergences between the calculation and the experiment for these assemblies are given in Table 9.

Table 9: Critical assemblies with an iron reflector

Experiment index from the Handbook	Location carried out	Geometry; reflector thickness	(k_c-k_e) in %, KENO ABBN-93	(k_c-k_e) in %, MCNP ENDF/B-V	(k_c-k_e) in %, MCNP ENDF/B-VI
IEU-MET-FAST-005	VNIIEF	Sphere (36%); reflector 8.25 cm	–0.02±0.21(7)	+1.35(6)	+0.00(6)
HEU-MET-FAST-021	VNIIEF	Sphere (90%); reflector 9.7 cm	–0.66±0.24(7)	+0.70(6)	–0.52(6)
PU-MET-FAST-025	VNIIEF	Sphere (2% ^{240}Pu); reflector 1.55 cm	–0.93±0.20(9)	+0.67(7)	–0.34(6)
PU-MET-FAST-032	VNIIEF	Sphere (10% ^{240}Pu); reflector 4.5 cm	–1.03±0.20(9)	–0.02(6)	–0.30(6)
PU-MET-FAST-026	VNIIEF	Sphere (2% ^{240}Pu); reflector 11 cm	–0.69±0.24(9)	+0.92(6)	–0.11(6)
PU-MET-FAST-028	VNIIEF	Sphere (2% ^{240}Pu); reflector 20 cm	–0.33±0.22(8)	+0.23(6)	–0.23(6)
PU-MET-FAST-015	IPPE[3]	BR-1 reactor with iron shielding	–0.06±0.27(8)	+0.17 (7)	
Expected root-mean-square spread (δk_{exp})			±0.24	±0.23	±0.21
Observed mean divergence ($\Delta k \pm \delta k_{cal}$)			-0.56±0.38	+0.58±0.46	-0.25±0.17

---

[3]   Institute of Physics and Power Engineering.

The data in the table show that only the calculations using the ENDF/B-VI constants describe the experimental data to an accuracy within the error levels. However, it should be remembered that the ENDF/B-VI constants did not prove similarly reliable in the analysis of the uranium and plutonium assemblies with no reflector. Therefore, for the iron reflector it is particularly important to examine the divergences between the calculated and experiment for the efficiency of the reflector, as was done above for the uranium and polyethylene reflectors. It should be borne in mind that calculating the efficiency of the iron reflector requires that the space dependence of resonance self-shielding of the iron cross-sections be taken into account. In the calculations using the MCNP program, this is done via a detailed description of the energy dependence of the neutron cross-sections in the resolved resonance region. In the calculations using the KENO program, the space dependence of resonance self-shielding is taken into account by using a large number of narrow energy groups, which allows the structure of the cross-sections in the vicinity of the strong *s*-resonances to be described in some detail. The unresolved resonance structure in the 299-group approximation (contribution of narrow *p*-resonances, the resonances at high energies, etc.) was taken into account using self-shielding factors, i.e. on average, without taking into account the space dependence of the self-shielding effect. Consequently, the albedo of the iron reflector may be slightly underestimated.

Table 10 gives data on the divergences between the calculated and experimental values for the efficiency of iron reflectors.

Table 10: Efficiency of iron reflectors

Experiment index from the Handbook	Location carried out	Geometry; reflector thickness	$(\delta k_{Fe,c}-\delta k_{Fe,e})$ in %, KENO ABBN-93	$(\delta k_{Fe,c}-\delta k_{Fe,e})$ in %, MCNP ENDF/B-V	$(\delta k_{Fe,c}-\delta k_{Fe,e})$ in %, MCNP ENDF/B-VI
IEU-MET-FAST-005 [basis IMF-003]	VNIIEF	Sphere (36%); reflector 8.25 cm	−0.10±0.25(9)	+0.81(8)	−0.46(8)
HEU-MET-FAST-021 [basis HMF-018]	VNIIEF	Sphere (90%); reflector 9.7 cm	−0.52±0.25(9)	+0.86 (9)	−0.15(8)
PU-MET-FAST-025 [basis PMF-022]	VNIIEF	Sphere (2% ^{240}Pu); reflector 1.55 cm	−0.66±0.30(11)	+1.02 (10)	+0.07(9)
PU-MET-FAST-032 [basis PMF-029]	VNIIEF	Sphere (10% ^{240}Pu); reflector 4.5 cm	−0.50±0.30(10)	+0.54 (10)	+0.11(9)
PU-MET-FAST-026 [basis PMF-022]	VNIIEF	Sphere (2% ^{240}Pu); reflector 11 cm	−0.42±0.30(9)	+1.27 (10)	+0.30(9)
PU-MET-FAST-028 [basis PMF-029]	VNIIEF	Sphere (2% ^{240}Pu); reflector 20 cm	+0.20±0.30(10)	+0.79 (10)	+0.18(10)
Expected root-mean-square spread (δk_{exp})			±0.30	±0.30	±0.28
Observed mean divergence ($\Delta k \pm \delta k_{cal}$)			-0.33±0.28	+0.88±0.21	+0.01±0.25

As may be seen from the above data, the ENDF/B-VI constants undoubtedly predict the efficiency of the iron reflector better than ENDF/B-V (use of the latter library causes significant overestimation of reflector efficiency). The ABBN-93 constants yield a reflector efficiency which is slightly lower than the experimental value, but this difference is significantly smaller than the error level of the experiment.

8. Conclusions

The fulfilled analysis shows that the calculations using the ABBN-93 constants underestimate k_{eff} for bare plutonium assemblies by -0.3±0.2%, and k_{eff} for uranium-233 spheres by -0.4±0.2%. No correlation of the divergence with the plutonium-240 content was observed. For bare high-enriched uranium assemblies, the calculated values of k_{eff} were also on average -0.25% lower than the experimental values but, since the root-mean-square spread of the experimental data has the same value, we may assume that the results of the calculations agree with the experimental data to within error limits.

The calculations with the ABBN-93 constants can be used to describe the efficiency of reflectors made of metallic uranium-238, iron and polyethylene and water to an accuracy within the experimental error levels.

REFERENCES

[1] MANTUROV, G.N., NIKOLAEV, M.N., TSIBOULIA, A.M., "BNAB-93 Group Data Library. Part 1: Nuclear Data for Calculation of Neutron and Photon Radiation Fields", INDC (CCP)-409/L, IAEA, Vienna (1997), 65-110.

[2] MANTUROV, G.N., NIKOLAEV, M.N., TSIBOULIA, A.M., "The ABBN-93 Group Constants System: Verification Report No. 1", State Information Service, Moscow (1995).

[3] International Handbook of Evaluated Criticality Safety Benchmark Experiments, OECD - Nuclear Energy Agency, NEA/NSC/DOC(95)03 (September 1997 Edition).

[4] CAPELL, B.M., MOSTELLER, R.D., PELOWITZ, D.B., "MCNP Calculations for Russian Criticality-Safety Benchmarks", Proceedings of the Topical Meeting on Criticality Safety Challenges in the Next Decade (September 7-11, Chelan, Washington), 384-392.

VALIDATION OF THE ABBN/CONSYST CONSTANTS SYSTEM.

PART 2: VALIDATION THROUGH THE CRITICAL EXPERIMENTS ON CORES WITH URANIUM SOLUTIONS

T.T. Ivanova, G.N. Manturov, M.N. Nikolaev, E.V. Rozhikhin,
M.YU. Semenov, A.M. Tsiboulia

State Scientific Centre of the Russian Federation - Institute for Physics
and Power Engineering, Obninsk

Abstract

VALIDATION OF THE ABBN/CONSYST CONSTANTS SYSTEM. P art 2:
Validation through the Critical Experiments on Cores with Uranium Solutions
Results of calculatins of critical asemblies with the cores of uranium solutions for
the considered series of the experiments are presented in this paper. The
conclusions about acceptability of the ABBN-93.1 cross sections for the
calculations of such systems are made

Introduction

By analysing homogeneous solution critical assemblies the usefulness of the constants
software system to be tested can be checked irrespective of how accurately this system takes
account of heterogeneous effects. As long as the criticality calculation in all the instances
below took detailed account of the geometry (in the majority of cases in a fairly simple form),
the divergences between the calculation and the experiment can only be due either to the
inaccuracy of the constants used for the calculation, or to the error levels of the evaluation of
the critical experiments. The calculations employing the ABBN constants were carried out in
a 299-group approximation using the KENO-Va program, and those employing ENDF/B-V

using the MCNP program. The calculation models for the experiments were based on the data given in the Handbook [1], and where the Handbook gave ready-made programs in the KENO-Va program language these were used directly. The calculations results using the MCNP program were, in the majority of cases, obtained by the authors of the evaluations and are taken from the Handbook [1].

1. Critical assemblies with high-enriched uranium solutions

The calculation results for critical assemblies with high-enriched uranium solutions are given in Table 1. In all cases the enrichment was at least 89% and is therefore not shown in the table. At the end of the table, as in Part 1, the mean characteristics of the divergences between the calculation and the experiment are given. The divergences between the experimental data and the calculation results are practically identical for both the ABBN-93 constants and ENDF/B-V.

Table 1: Critical assemblies with high enriched uranium solutions

Experiment index from the Handbook	Location carried out	Geometry and solution parameters	$(k_c\text{-}k_e)$, % KENO ABBN-93	$(k_c\text{-}k_e)$, % MCNP ENDF/B-V	$k(MCNP\text{-}BV)$- $k(KENO\text{-}93)$, %
Cylinders with no reflector HEU-SOL-THERM-001-1	Rocky Flats Plant	$\varnothing$27.9 cm (SS), h = 31.2 cm, C_U = 146 g/l	+0.25±0.25(10)	+0.47(21)	+0.22±0.23
HEU-SOL-THERM-001-2		$\varnothing$27.9 cm (SS), h = 28.9 cm, C_U = 367 g/l	+0.16±0.25(10)	+0.13(21)	-0.03±0.23
HEU-SOL-THERM-001-3		$\varnothing$28.0 cm (Al), h = 33.6 cm, C_U = 143 g/l	+0.73±0.25(11)	+0.64(20)	-0.09±0.23
HEU-SOL-THERM-001-4		$\varnothing$28.0 cm (Al), h = 30.9 cm, C_U = 358 g/l	**+0.88±0.25(11)**	+0.15(21)	-0.73±0.24
HEU-SOL-THERM-001-5		$\varnothing$33.0 cm (Al), h = 39.5 cm, C_U = 54.9 g/l	+0.19±0.25(9)	+0.27(16)	+0.08±0.18
HEU-SOL-THERM-001-6		$\varnothing$33.0 cm (Al), h = 36.7 cm, C_U = 59.7 g/l	+0.66±0.25(9)	+0.74(16)	+0.08±0.18
HEU-SOL-THERM-001-7		$\varnothing$33.0 cm (Al), h = 24.0 cm, C_U = 137.4 g/l	+0.19±0.25(10)	+0.51(20)	+0.32±0.22
HEU-SOL-THERM-001-8		$\varnothing$33.0 cm (Al), h = 23.7 cm, C_U = 145.7 g/l	+0.41±0.25(10)	+0.39(20)	-0.02±0.22
HEU-SOL-THERM-001-9		$\varnothing$33.0 cm (Al), h = 22.5 cm, C_U = 357.7 g/l	+0.37±0.25(11)	+0.06(22)	-0.31±0.25
HEU-SOL-THERM-001-10		$\varnothing$50.7 cm (Al), h = 20.5 cm, C_U = 64 g/l	-0.41±0.25(10)	-0.025(17)	+0.39±0.20

Experiment index from the Handbook	Location carried out	Geometry and solution parameters	(k_c-k_e), % KENO ABBN-93	(k_c-k_e), % MCNP ENDF/B-V	$k(MCNP\text{-}BV)-k(KENO\text{-}93)$, %
The same cylinders in the centre of a concrete cell 122x122x122 cm HEU-SOL-THERM-002-1	Rocky Flats Plant	$\varnothing$27.9 cm, h = 29.8 cm, C_U = 144.4 g/l	+0.55±0.20(10)	+0.47(21)	-0.08±0.23
HEU-SOL-THERM-002-3		$\varnothing$27.9 cm, h = 29.8 cm, C_U = 144.4 g/l	**+0.68±0.20(10)**	+0.66(24)	-0.02±0.26
HEU-SOL-THERM-002-9		$\varnothing$27.9 cm, h = 29.8 cm, C_U = 144.4 g/l	+0.33±0.20(9)	+0.66(23)	+0.33±0.25
The same cylinders in the centre of a plexiglass cell 123x123x123 cm HEU-SOL-THERM-003-3	Rocky Flats Plant	$\varnothing$27.9 cm (SS), h = 29.8 cm, C_U = 147.7 g/l	+0.36±0.50(10)	+0.73(25)	+0.37±0.27
HEU-SOL-THERM-003-5		$\varnothing$27.9 cm (SS), h = 27.6 cm, C_U = 345.33 g/l	+0.27±0.50(10)	+0.09(21)	-0.18±0.23
HEU-SOL-THERM-003-8		$\varnothing$28.1 cm (Al), h = 31.3 cm, C_U = 147.7 g/l	+0.69±0.50(10)	+0.65(23)	-0.04±0.25
HEU-SOL-THERM-003-10		$\varnothing$28.1 cm (Al), h = 28.8 cm, C_U = 345.3 g/l	+0.57±0.50(10)	0.00(23)	-0.57±0.25
HEU-SOL-THERM-003-12		$\varnothing$33.0 cm (Al), h = 34.3 cm, C_U = 60.3 g/l	+0.41±0.50(9)	+0.40(22)	-0.01±0.24
HEU-SOL-THERM-003-16		$\varnothing$33.0 cm (Al), h = 22.8 cm, C_U = 147.7 g/l	+0.31±0.50(10)	+0.27(23)	-0.04±0.25
HEU-SOL-THERM-003-18		$\varnothing$33.0 cm (Al), h = 21.7 cm, C_U = 345.3 g/l	+0.68±0.50(11)	-0.48(23)	**-1.16±0.25**
HEU-SOL-THERM-003-1	LANL	Cylinder $\varnothing$35.6 cm, h = 13.86 cm, C_U = 144.4 g/l	-1.10±0.50(10)	-1.05(14)	+0.05±0.17
HEU-SOL-THERM-003-8		The same with an H$_2$O reflector	-1.31±0.54(10)	-1.37(15)	-0.06±0.18
Sphere with UO$_2$F$_2$ solutions with an H$_2$O reflector HEU-SOL-THERM-009-1	ORNL	R = 11.52 cm (Al) C_U = 696.4 g/l	+1.16±0.57(10)	+0.44(7)	**-0.72±0.12**
HEU-SOL-THERM-009-2		R = 11.47 cm (Al) C_U = 543.0 g/l	+1.34±0.57(10)	+0.42(6)	**-0.92±0.12**
HEU-SOL-THERM-009-3		R = 11.52 cm (Al) C_U = 348.8 g/l	+0.88±0.57(10)	+0.60(7)	-0.28±0.12

Experiment index from the Handbook	Location carried out	Geometry and solution parameters	$(k_c - k_e)$, % KENO ABBN-93	$(k_c - k_e)$, % MCNP ENDF/B-V	$k(MCNP\text{-}BV)$- $k(KENO\text{-}93)$, %
HEU-SOL-THERM-009-4		R = 11.84 cm (Al) C_U = 213.2 g/l	+0.08±0.57(10)	-0.12(7)	-0.20±0.12
Sphere with UO$_2$F$_2$ solutions with an H$_2$O reflector HEU-SOL-THERM-010-1	ORNL	R = 13.2 cm (Al) C_U = 102.6 g/l; T = 27.5ºC	+0.46±0.18(9)	+0.40(7)	-0.06±0.11
HEU-SOL-THERM-010-2		R = 13.2 cm (Al) C_U = 103.8 g/l; T = 39.5ºC	**+0.65±0.18(10)**	+0.55(7)	-0.10±0.12
HEU-SOL-THERM-010-3		R = 13.2 cm (Al) C_U = 109.4 g/l; T = 74.0ºC	+0.38±0.18(9)	+0.40(7)	+0.02±0.11
HEU-SOL-THERM-010-4		R = 13.2 cm (Al) C_U = 111.5 g/l; T = 85.5ºC	+0.12±0.18(9)	+0.15(7)	+0.03±0.11
Sphere with UO$_2$F$_2$ solutions with an H$_2$O reflector HEU-SOL-THERM-011-1	ORNL	R = 17.0 cm (Al) C_U = 53.0 g/l	+0.62±0.20(8)	+0.83(5)	+0.21±0.09
HEU-SOL-THERM-011-2		R = 17.2 cm (Al) C_U = 52.1 g/l	+0.17±0.20(8)	+0.44(5)	+0.27±0.09
HEU-SOL-THERM-012-1 Sphere with UO$_2$F$_2$ solution with an H$_2$O reflector	ORNL	R = 27.9 cm (Al) C_U = 21.4 g/l	+0.05±0.58(6)	+0.37(5)	+0.32±0.08
HEU-SOL-THERM-013-1 Sphere with uranyl nitrate solutions with no reflector	ORNL	R = 34.6 cm (Al) C_U = 20.12 g/l	-0.31±0.26(6)	+0.01(4)	+0.32±0.07
HEU-SOL-THERM-013-2		R = 34.6 cm (Al) C_U = 23.53 g/l	-0.36±0.36(6)	-0.09(4)	+0.27±0.07
HEU-SOL-THERM-013-3		R = 34.6 cm (Al) C_U = 26.77 g/l	-0.51±0.36(6)	-0.40(4)	+0.11±0.07
HEU-SOL-THERM-013-4		R = 34.6 cm (Al) C_U = 28.45 g/l	-0.39±0.36(6)	-0.29(4)	+0.10±0.07
HEU-SOL-THERM-014-1	IPPE	Cylinder ∅40 cm, h = 19.3 cm with reflector C_U = 70 g/l	-0.51±0.27(9)	-0.31(19)	+0.27±0.21
HEU-SOL-THERM-015-1	IPPE	Cylinder ∅40 cm, h = 18.7 cm with reflector C_U = 100 g/l	-0.24±0.27(9)	+0.37(23)	+0.64±0.25
HEU-SOL-THERM-015-2 (Different reflector configuration)		Cylinder ∅40 cm, h = 16.6 cm with reflector C_U = 100 g/l	**-1.17±0.34(9)**	-0.35(21)	+0.57±0.23
HEU-SOL-THERM-016-1	IPPE	Cylinder ∅40 cm, h = 15.1 cm with reflector C_U = 156.5 g/l	-1.05±0.36(10)	-0.14(22)	+0.66±0.24

Experiment index from the Handbook	Location carried out	Geometry and solution parameters	(k_c-k_e), % KENO ABBN-93	(k_c-k_e), % MCNP ENDF/B-V	$k(MCNP\text{-}BV)-k(KENO\text{-}93)$, %
HEU-SOL-THERM-017-1	IPPE	Cylinder $\varnothing$24.8 cm, h = 22.6 cm with reflector C_U = 202 g/l	-0.55±0.28(10)	+0.16(23)	+0.01±0.25
HEU-SOL-THERM-017-2		Cylinder $\varnothing$40.0 cm, h = 15.6 cm with reflector C_U = 202 g/l	**-1.69±0.40(10)**	-1.41(25)	+0.13±0.27
HEU-SOL-THERM-017-3 (Different from the preceding reflector configuration)		Cylinder $\varnothing$40.0 cm, h = 14.3 cm with reflector C_U = 202 g/l	**-1.95±0.36(10)**	-1.09(23)	+0.36±0.25
HEU-SOL-THERM-018-1	IPPE	Cylinder $\varnothing$24.8 cm, h = 21.7 cm with reflector C_U = 300 g/l	-0.57±0.34(10)	-1.12(21)	-0.15±0.23
HEU-SOL-THERM-018-2		Cylinder $\varnothing$40.0 cm, h = 50.5 cm with reflector C_U = 300 g/l	-1.18±0.46(10)	-0.83(25)	+0.15±0.27
HEU-SOL-THERM-018-3 (Different from the preceding reflector configuration)		Cylinder $\varnothing$40.0 cm, h = 14.3 cm with reflector C_U = 300 g/l	-0.81±0.42(10)	-1.70(24)	-0.08±0.26
HEU-SOL-THERM-019-1	IPPE	Cylinder $\varnothing$24.8 cm, h = 22.6 cm with reflector C_U = 447 g/l	+0.34±0.40(10)	+0.08(23)	-0.16±0.25
HEU-SOL-THERM-025-1	IPPE	Cylinder $\varnothing$40.0 cm, h = 23.8 cm with reflector C_U = 51.2 g/l	+0.01±0.25(8)	+0.31(8)	+0.30±0.11
HEU-SOL-THERM-025-2 (Different from the preceding reflector configuration)		Cylinder $\varnothing$40.0 cm, h = 23.8 cm with reflector C_U = 51.2 g/l	-0.02±0.25(8)	+0.31(8)	+0.33±0.11
HEU-SOL-THERM-025-4		Cylinder $\varnothing$40.0 cm, h = 23.1 cm with reflector C_U = 53 g/l	+0.06±0.27(8)	+0.66(8)	**+0.60±0.11**
HEU-SOL-THERM-025-5		Cylinder $\varnothing$40.0 cm, h = 18.8 cm with reflector C_U = 77 g/l	+0.11±0.30(8)	+0.67(9)	**+0.56±0.12**
Expected root-mean-square spread (δk_{exp})			±0.30	±0.33	±0.20
Observed mean divergence ($\Delta k \pm \delta k_{cal}$)			+0.12±0.57	+0.23±0.51	**+0.04±0.37**

As may be seen, the calculations agree well on average with the experimental data. However, the root-mean-square spread was one and a half to two times higher than expected using either of the constants systems under consideration. Hence it follows that the value

$\pm\,0.3\%$ can hardly be viewed as a realistic evaluation of the mean error level of one experiment. There is every reason for assuming that the experimenters underestimated the error levels and, most probably, that systematic error common to the whole series of experiments was not taken into account. Figure 2 shows the divergences between the calculation and the experiment as a function of the uranium concentration. There is clearly no statistically significant dependence either in the calculations using the ABBN-93 constants (circles) or in those using ENDF/B-V (crosses).

At the same time it is clear that the results obtained for an identical uranium concentration in the solution (i.e. within one experimental series) deviate from the calculated values in one direction if not as a rule, then often. The important point here, however, is not the concentration of the solution but that the experiments belong to the same series. Thus, in the HEU-SOL-THERM-002 and -003 experiments, almost all the k_{eff} values were below the calculated values, even though the concentration ranged from 50 to 350 g/l. Both results in the HEU-SOL-THERM-006 experiment are significantly higher than the calculated values. Also higher than the calculated values were the majority of the data measured at the IPPE in series HEU-SOL-THERM-014, ... , -019, -025.
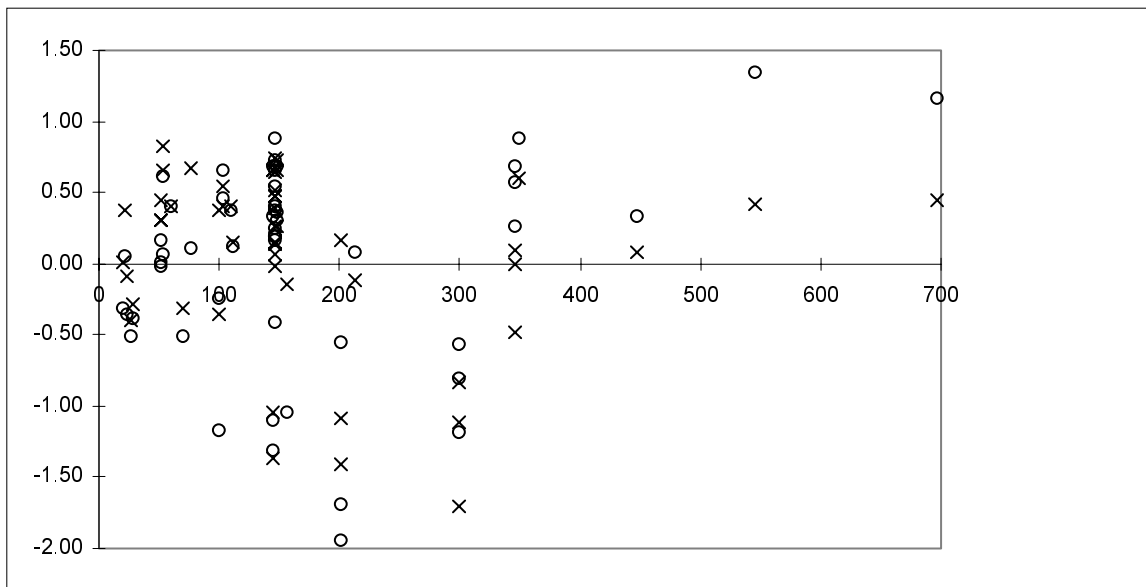

Fig. 1. Divergences between the calculation and experiment in dependence on the uranium concentration in the solution. Solution critical experiments with high-enriched uranium are considered. Circles - calculations using KENO-CONSYST; crosses - calculations using MCNP-ENDF/B-V.

Owing to the presence of unidentified systematic errors (i.e. strongly correlated for the results of one series), the root-mean-square spread would seem to be a more realistic evaluation of the mean error level of one experiment. However, even using this more cautious evaluation, in view of the lack of any systematic dependence for the divergences on concentration it is hardly possible to view all 52 experiments as independent measurements of the same value (k_{eff} of the high enriched uranyl nitrate solution) and take the mean error level of the calculated result to be $\pm 0.6/\sqrt{52} \approx \pm 0.08\%$. This evaluation would be unduly optimistic. It would be more realistic to divide by the square root of the number of experimental series (there are 16 of them). In this case, we would have to adopt an error level of $\pm 0.15\%$ for the calculated prediction of k_{eff} for solution systems similar to those above. However, even this error level is unduly optimistic since it can be applied with equal success to calculations employing both ABBN-93 and ENDF/B-V, though the results of these calculations (they are compared with one another in the last column of Table 1) diverge on average from one another by only 0.04%, whereas their root-mean-square spread is 0.37% which is twice as high as the divergence which would be expected on the basis of the statistical error level of the calculated results. This wide spread is caused by certain anomalously high divergences between calculation results for comparable systems. In six cases the divergences between the results of comparable calculations exceed the statistical error level by a factor of more than 3. These divergences are bolded in Table 1. Thus, for example, in the HEU-SOL-THERM-003 series, at a uranium concentration of 345.3g/l, when the tank diameter is increased from 28cm to 33cm the error level of the calculations using KENO-CONSYST rises from +0.2% to +0.7%, whereas the divergence from the calculations employing MCNP-ENDF/B-V moves in the opposite direction - from +0.1% to -0.5%, so the divergence between these calculations for the experiment with a tank radius of 33cm is 1.2%. In the same experimental series, at a uranium concentration of 147.7g/l, the divergences in the calculated results do not significantly exceed the statistical error level (which is $\pm 0.27\%$ for the difference in the calculated results). It should be noted that, on comparing the results obtained using the KENO program with the ABBN-93 and ENDF/B-IV constants, similar large differences are not observed: the divergences do not exceed the statistical error levels either in the above-mentioned HEU-SOL-THERM-003 series of experiments or in the HEU-SOL-THERM-009 series of experiments where, for variants 1 and 2, the divergences between the calculations using KENO-CONSYST and MCNP-ENDF/B-V are anomaly high. One possible cause of the anomalous divergences noted is hidden errors in the calculation programs. If this is in fact the case, after these errors have been identified and eliminated we might expect the calculation results for comparable constants software packages to agree with one another to within statistical error limits. In this case, the evaluation of $\pm 0.15\%$ for the error level of calculated k_{eff} would acquire credibility.

Until the causes of the anomalous divergences found is clarified, on the basis of the above data we can assert at this point that, in future high-accuracy critical experiments on high-enriched uranium solutions, we can expect that the divergence from the calculated results using any of the above constants systems will not exceed 0.5%, if there are no errors in the calculation programs.

2. Critical assemblies with low-enriched uranium solutions

There are relatively few experimental data on criticalities of low-enriched uranium solutions. All the data included in the Handbook were analysed and the results are given in Table 2 below. Essentially, data are available for two enrichment levels only - 10% and 5%. The experiment with a 29% uranyl nitrate solution in a graphite reflector (IEU-SOL-THERM-001) was not taken into account here owing to the particularly complex geometry and the lack of any description of this geometry in the input language of the KENO program. Divergences (and agreement) between the calculation and the experiment under identical experimental conditions with a complex description can always be attributed to incorrect programming.

Table 2:   Critical assemblies with low-enriched uranium solutions

Experiment index from the Handbook	Location carried out	Geometry and solution parameters	$(k_c\text{-}k_e)$, % KENO ABBN-93	$(k_c\text{-}k_e)$, % MCNP ENDF/B-V	$k(CNP\text{-}BV)\text{-}k(KENO\text{-}93)$, %
Spheres with no reflector, enrichment 10.2%; D = 65.9 cm; LEU-SOL-THERM-003-1	IPPE	D = 65.9 cm; truncated: h/D = 0.749; C_U = 296 g/l.	-0.16 ±0.39(7)	-0.06(4)	+0.1±0.08
LEU-SOL-THERM-003-2		D = 65.9 cm; truncated: h/D = 0.882; C_U = 264 g/l.	-0.42±0.42(7)	-0.12(4)	+0.3±0.08
LEU-SOL-THERM-003-3		D = 65.9 cm; full: h/D = 1.000; C_U = 260 g/l	+0.33±0.42(6)	+0.25(4)	-0.08±0.07
LEU-SOL-THERM-003-4		D = 87.3 cm; truncated: h/D = 0.545; C_U = 255 g/l	-0.58±0.42(7)	-0.52(4)	+0.06±0.08
LEU-SOL-THERM-003-5		D = 87.3 cm; truncated: h/D = 0.821; C_U = 203 g/l	-0.37±0.48(5)	-0.14(3)	+0.23±0.06
LEU-SOL-THERM-003-6		D = 87.3 cm; full: h/D = 1.000; C_U = 197 g/l	-0.22±0.49(5)	-0.12(3)	+0.10±0.06

Experiment index from the Handbook	Location carried out	Geometry and solution parameters	$(k_c\text{-}k_e)$, % KENO ABBN-93	$(k_c\text{-}k_e)$, % MCNP ENDF/B-V	$k(CNP\text{-}BV)$- $k(KENO\text{-}93)$, %
LEU-SOL-THERM-003-7		D = 119.8 cm; truncated: h/D = 0.538; C_U = 193 g/l	-0.40±0.49(5)	-0.25(3)	+0.15±0.06
LEU-SOL-THERM-003-8		D = 119.8 cm; truncated: h/D = 0.850; C_U = 171 g/l	-0.05±0.52(5)	+0.07(3)	+0.12±0.06
LEU-SOL-THERM-003-9		D = 119.8 cm; full: h/D = 1.000; C_U = 168 g/l	-0.29±0.52(5)	-0.17(3)	+0.12±0.06
LEU-SOL-THERM-001-1	LANL	Cylinder (∅25cm) with uranium oxy-fluoride solution (5%) with no reflector; C_U = 1000 g/l	**+1.18±0.29(8)**	**+1.014(10)**	-0.17±0.13
LEU-SOL-THERM-002-1	ORNL	Sphere (∅ 69 cm) with uranium oxy-fluoride solution (4.9%) with an H_2O reflector; C_U = 450 g/l	-0.54±0.40(5)	-0.32(4)	+0.22±0.06
LEU-SOL-THERM-002-2		The same with no reflector, C_U = 492 g/l	-0.71±0.37(6)	-0.61(4)	+0.1±0.07
LEU-SOL-THERM-003-2		Truncated sphere with reflector H/D =0.740; C_U = 492 g/l	-0.34 ±0.44(6)	-0.12(4)	+0.22±0.07
Expected root-mean-square spread (δk_{exp})			±0.42	±0.42	**±0.08**
Observed mean divergence ($\Delta k \pm \delta k_{cal}$)			-0.10±0.17 -0.33±0.08*	±0.13 -0.20±0.09*	**+0.11±0.12** **+0.14**±0.09*

*   The averaging results do not include the data from experiment LEU-SOL-THERM-001.

In Table 2 there is a satisfactory level of agreement between the calculated results and the experimental data on average. However, the fact that only two of the 13 experiments used yielded a k_{eff} value higher than the calculated value, and that the positive contribution of these two experiments (+0.2) was only a little less than the total negative contribution of the remaining 11 experiments (-0.3) is disturbing. This also caused the low mean divergence value. As was the case with the high enriched uranium solutions, there is every reason to assume that the experimental data contain systematic errors which are most probably common to experiments in the same series. Indeed, all three experiments carried out at ORNL and eight of the nine experiments carried out at IPPE yielded results higher than the calculated results, though they do agree with the calculation to within error limits; on the other hand, the experiment carried out at LANL yielded a k_{eff} value more than 1% lower than the calculated values. The fact that the root-mean-square spread of the data is significantly smaller than would be expected from the evaluated experimental error levels (assuming that these error levels are not correlated) would also indicate that there is systematic error. If experiment LEU-SOL-THERM-001 (whose result differs most markedly from the calculated data) is excluded, the mean divergences do rise, but they are still less than the divergences which would be expected from the evaluated experimental error levels (see Table 2 - mean values marked with an asterisk). The difference in the mean divergences (0.2%) calculated taking into account all the experiments except the one which differs most markedly from the calculated data can be taken as a measure of the error level of the calculated results.

It should be noted that, in contrast to the experiments with high-enriched uranium solutions, no unexpectedly high differences between the calculations using KENO-CONSYST and those using MCNP-ENDF/B-V were observed for this series of experiments: the mean divergence between them - expressed as a percentage of k_{eff} - is 0.11±0.12, and the maximum differences are only 0.22-0.23%.

3. Critical assemblies with uranium-233 solutions

The results of only two series of critical experiments on uranium-233 solutions have been published. Series U233-SOL-THERM-001 determined the dependence of the critical concentration on the boron additive levels. In all cases the additive level was fairly low, so the majority of fissions occurred in the thermal energy region. Series U233-SOL-THERM-008 included only one experiment on a uranium-233 solution with no absorber added. The calculation results are compared with the experimental data in Table 3.

Above all, the data in Table 3 show that calculations using the ABBN-93 constants underestimate k_{eff} by 0.7-0.8%, whereas the ENDF/B-V constants yield an excellent level of agreement with the experimental data. No dependence of the divergence on the boron concentration was found (which was to be expected considering the fact that, even at the maximum boron concentration, the vast majority of fissions and neutron absorptions were occurring in the thermal region (below 0.46 eV)). Attention is drawn to the correlation of the error levels for the results of the five experiments in the first series. This is understandable since the descriptions of the experimental data clearly show that the main sources of experimental error were inaccurate knowledge of the uranium concentration in the solution and the density of the solution; an error level of ±0.5% was ascribed to each of these, which is

at least twice as high as the spread of the measurement results relative to the continuous curve (straight line) drawn through them. The error level for the volume of the sphere also appears to be common to all these experiments, although its contribution is small. Owing to this correlation, it would seem wise to average only the results of the first and last experiments whose error levels, even though they are correlated, are of course much lower than the error levels of the other experiments belonging to the first series. As can be seen from the data in Table 3, this does not affect the nature and scale of the divergences.

The preferability of ENDF/B-V over the [233]U constants used in ABBN-93 was also apparent in the study of the metallic spheres, though not quite so clearly (see section 1.4). It would therefore seem wise to recalculate the ABBN constants using the ENDF/B-V data.

Table 3:   Critical assemblies with Uranium-233 solutions

Experiment index from the Handbook	Location carried out	Geometry and solution parameters	(k_c-k_e) %, KENO ABBN-93	(k_c-k_e) %, MCNP ENDF/B-V	$k(MCNP\text{-}BV)-k(KENO\text{-}93)$, %
U233-SOL-THERM-001-1	ORNL	Aluminium sphere D=70 cm with no reflector U concentration = 16.76 g/l B concentration = 0	+0.94±0.31(6)	+0.13(5)	-0.81(8)
U233-SOL-THERM-001-2		U concentration = 17.42 g/l B concentration = 0.0233 g/l	+0.92±0.33(5)	+0.08(5)	-0.83(7)
U233-SOL-THERM-001-3		U concentration = 18.03 g/l B concentration = 0.0453 g/l	+0.85±0.33(6)	+0.06(6)	-0.79(8)
U233-SOL-THERM-001-4		U concentration = 18.67 g/l B concentration = 0.0670 g/l	+0.91±0.33(6)	+0.03(6)	-0.88(8)
U233-SOL-THERM-001-5		U concentration = 19.27 g/l B concentration = 0.0887 g/l	+0.90±0.33(6)	+0.00(6)	-0.90(8)
U233-SOL-THERM-008	ORNL	U concentration = 13.05 g/l	+0.46±0.29(4)	-0.21(4)	-0.67(6)
Expected root-mean-square spread (Δk_{exp})			±0.32	±0.32	±0.08
Observed mean divergence ($\Delta k \pm \delta k_{cal}$)			+0.83±0.17 +0.70±0.24[*]	+0.02±0.10 -0.04±0.17[*]	-0.81±0.07

*   Averaging results for only the first and last experiments (with no boron).

8.   Conclusions

The analysis shows that the results of the calculations for critical assemblies with high-enriched uranium agree well on average with the experimental data.

In the series of experiments with low-enriched uranium solutions, the difference in the mean divergences of 0.2% calculated taking into account all the experiments except the one which differed most markedly from the calculated data represents a satisfactory level of agreement between the calculation results using the ABBN-93 constants and the experimental data on average. In this series of experiments, the calculations using ABBN-93 and ENDF/B-V show a high level of agreement with one another: the mean divergence between them - expressed as a percentage of k_{eff} - is 0.11-0.12.

The calculations for critical assemblies with ^{233}U solutions using the ABBN-93 constants underestimate k_{eff} by 0.7-0.8%. The preferability of ENDF/B-V over the ^{233}U constants in ABBN-93 indicates that it would be wise to recalculate the ABBN constants using the ENDF/B-V data.

REFERENCES

[1]   International Handbook of Evaluated Criticality Safety Benchmark Experiments. OECD - Nuclear Energy Agency, NEA/NSC/DOC(95)03 (September 1997 Edition).

.